





OPEN ACCESS

Original research

Protective function of sclerosing cholangitis on IBD

Tanja Bedke ^{1,2}, Friederike Stumme,^{1,2} Miriam Tomczak,^{1,2} Babett Steglich,^{1,2} Rongrong Jia,^{1,2} Simon Bohmann,¹ Agnes Wittek,¹ Jan Kempinski,^{1,2} Emilia Göke,^{1,2} Marius Böttcher,^{1,2} Dominik Reher,¹ Anissa Franke,^{1,2} Maximilian Lennartz,^{3,4} Till Clauditz,^{3,4} Guido Sauter,^{3,4} Thorben Fründt,⁵ Sören Weidemann,³ Gisa Tiegs,⁶ Christoph Schramm,^{2,5,7} Nicola Gagliani,^{1,2} Penelope Pelczar,^{1,2} Samuel Huber ^{1,2}

► Additional supplemental material is published online only. To view, please visit the journal online (<https://doi.org/10.1136/gutjnl-2023-330856>).

For numbered affiliations see end of article.

Correspondence to

Professor Samuel Huber, I. Department of Medicine, University Medical Center Hamburg-Eppendorf, Hamburg 20246, Germany; shuber@uke.de

TB, FS and MT are joint first authors.
PP and SH are joint senior authors.

Received 4 August 2023
Accepted 9 May 2024

ABSTRACT

Objective There is a strong clinical association between IBD and primary sclerosing cholangitis (PSC), a chronic disease of the liver characterised by biliary inflammation that leads to strictures and fibrosis. Approximately 60%–80% of people with PSC will also develop IBD (PSC-IBD). One hypothesis explaining this association would be that PSC drives IBD. Therefore, our aim was to test this hypothesis and to decipher the underlying mechanism.

Design Colitis severity was analysed in experimental mouse models of colitis and sclerosing cholangitis, and people with IBD and PSC-IBD. Foxp3⁺ Treg-cell infiltration was assessed by qPCR and flow cytometry. Microbiota profiling was carried out from faecal samples of people with IBD, PSC-IBD and mouse models recapitulating these diseases. Faecal microbiota samples collected from people with IBD and PSC-IBD were transplanted into germ-free mice followed by colitis induction.

Results We show that sclerosing cholangitis attenuated IBD in mouse models. Mechanistically, sclerosing cholangitis causes an altered intestinal microbiota composition, which promotes Foxp3⁺ Treg-cell expansion, and thereby protects against IBD. Accordingly, sclerosing cholangitis promotes IBD in the absence of Foxp3⁺ Treg cells. Furthermore, people with PSC-IBD have an increased Foxp3⁺ expression in the colon and an overall milder IBD severity. Finally, by transplanting faecal microbiota into gnotobiotic mice, we showed that the intestinal microbiota of people with PSC protects against colitis.

Conclusion This study shows that PSC attenuates IBD and provides a comprehensive insight into the mechanisms involved in this effect.

INTRODUCTION

IBD is characterised by chronic relapsing intestinal inflammation. The exact aetiology of IBD is not completely understood, but it is known that IBD is characterised by chronic inflammation, intestinal dysbiosis and mucosal barrier defects. Thus, one hypothesis is that IBD is a result of an aberrant immune response against intestinal bacteria in genetically susceptible individuals.^{1–3} There is a strong clinical association between IBD and primary sclerosing cholangitis (PSC), a chronic, cholestatic liver disease characterised by inflammation and fibrosis of the bile ducts inside and outside the liver.

WHAT IS ALREADY KNOWN ON THIS TOPIC

⇒ There is a strong clinical association between IBD and primary sclerosing cholangitis (PSC). However, currently it is unknown, if this association is due to common genetic polymorphisms or if PSC may drive IBD.

WHAT THIS STUDY ADDS

⇒ Unexpectedly, we found that PSC attenuates IBD. Mechanistically, PSC causes an altered intestinal microbiota composition, which promotes Foxp3⁺ Treg-cell expansion, and thereby protects against IBD.

HOW THIS STUDY MIGHT AFFECT RESEARCH, PRACTICE OR POLICY

⇒ We believe that our data build a basis for the development of new therapeutical strategies targeting the microbiota-Foxp3⁺ Treg-cell axis in IBD.

Approximately 60%–80% of people with PSC have concomitant IBD (from here on referred to as PSC-IBD).^{1,4} Conversely, only about 5% of people with IBD will develop PSC during their disease course.² Notably, people suffering from PSC-IBD have a phenotype distinct from Crohn's disease (CD) and Ulcerative colitis (UC), characterised by an overall milder IBD severity, a higher prevalence of right-sided predominant pancolitis, rectal sparing, backwash ileitis and an increased risk of developing colorectal neoplasia.^{3,5} Even for people with PSC without clinically manifested IBD, we have previously shown that a high proportion exhibits molecular signs of intestinal inflammation, characterised by immune cell infiltration and expression of proinflammatory cytokines in intestinal biopsies.⁶

The factors that contribute to the development of PSC-IBD are not yet understood. Previous studies suggest a critical role of CD4⁺ Foxp3⁺ regulatory T cells (Foxp3⁺ Treg) in IBD, as well as PSC.^{7–9} In line with these data, reduced Foxp3⁺ Treg-cell numbers and function were associated with single nucleotide polymorphisms in the *IL2RA* gene present in people with IBD and PSC.^{10–12} Interestingly, the microbiota plays a key role in the emergence of Foxp3⁺ Treg cells: microbiota-derived short-chain fatty acids (SCFAs) can facilitate the induction of Foxp3⁺ Treg



© Author(s) (or their employer(s)) 2024. Re-use permitted under CC BY. Published by BMJ.

To cite: Bedke T, Stumme F, Tomczak M, *et al.* Gut Epub ahead of print: [please include Day Month Year]. doi:10.1136/gutjnl-2023-330856

cells both in *in vitro* and in animal models.^{13,14} Accordingly, aside from genetic predispositions in genes regulating Foxp3⁺ Treg-cell function, the intestinal microbiota has been suggested to be one of the contributing factors for the close association of IBD and PSC.¹⁵ Indeed, both IBD and PSC are characterised by intestinal dysbiosis. Moreover, direct comparisons revealed distinct microbiota compositions between these diseases.^{16–22} Thus, among others, the phylae *Veillonella* and *Escherichia* have been reported to be enriched in people with PSC-IBD compared with IBD alone, that are proposed to promote immune cell migration to the gut. In addition, bacteria of the *Lachnospiraceae* family which produce anti-inflammatory SCFAs were reported to be increased in people with PSC.²³ However, it remains unclear, whether changes in the microbial composition caused by PSC lead to an altered Foxp3⁺ Treg-cell expansion and function that contributes to the phenotype of IBD in people with PSC.

Taken together, there is a clear connection between IBD and PSC. However, whether PSC increases the risk for IBD but attenuates its phenotype remains to be elucidated. In this study we combined cellular and microbial analyses from experimental mouse models of colitis and sclerosing cholangitis, biopsies and stool samples of people with PSC-IBD and IBD, and then performed human faecal microbiota transplantation (FMT) into gnotobiotic mice to decipher the impact of PSC on IBD.

RESULTS

Experimental sclerosing cholangitis attenuates colitis severity and increases Foxp3⁺ Treg-cell frequency in mice

First, we aimed to test the connection between IBD and sclerosing cholangitis in experimental mouse models. To this end, *Il10*^{-/-} mice, which develop spontaneous colitis²⁴ were crossed to *Mdr2*^{-/-} mice, a mouse model for experimental sclerosing cholangitis²⁵ (figure 1A). As expected, *Il10*^{-/-}*Mdr2*^{-/-} mice, but not *Il10*^{-/-} mice, developed sclerosing cholangitis based on increased transaminase AST and ALT levels, and fibrosis score (online supplemental figure S1A,B). Next, we assessed IBD severity. We found that *Il10*^{-/-} and *Il10*^{-/-}*Mdr2*^{-/-} mice developed an overall mild colitis (figure 1B,C). Interestingly, *Il10*^{-/-}*Mdr2*^{-/-} mice with a concomitant experimental sclerosing cholangitis developed significantly reduced colitis compared with *Il10*^{-/-} mice (figure 1C). However, there was little impact on weight, despite the differences observed in colitis severity using endoscopy. Of note, we aimed to induce a mild to moderate colitis severity in our experiments in order to limit the suffering of the animals. Thus, all mice showed a relatively mild weight loss, and we therefore may have not observed a difference. Moreover, while colonic CD4⁺ T-cell infiltration was comparable between the groups (figure 1D), the proportion of Foxp3⁺ Treg cells within the CD4⁺ T-cell population was significantly increased in the inflamed colon of *Il10*^{-/-}*Mdr2*^{-/-} compared with *Il10*^{-/-} mice (figure 1D,E).

The intestinal microbiota composition is known to impact colitis-susceptibility²⁶. Therefore the colitis development we observed in *Il10*^{-/-} mice under specific pathogen-free (SPF) conditions of the local mouse facility (referred to as MB1) was generally mild. To this end, we next aimed to determine spontaneous colitis development in *Il10*^{-/-} mice bred in the presence of a colitogenic SPF microbiota, that showed a distinct beta diversity compared with MB1, including an enrichment of *Helicobacter* on genus level (referred to as MB2) (online supplemental figure S2A,B; figure 1F). As expected, the mice bred under MB2 conditions showed an overall increased susceptibility to developing colitis compared with mice with MB1 microbiota

(figure 1C,H). Comparisons between *Il10*^{-/-} and *Il10*^{-/-}*Mdr2*^{-/-} mice bred under MB2 conditions revealed no differences in body weight between the groups (figure 1G). However, colitis severity in *Il10*^{-/-}*Mdr2*^{-/-} mice with concomitant sclerosing cholangitis (online supplemental figure S1C,D) was significantly reduced compared with *Il10*^{-/-} mice (figure 1H). Moreover, *Il10*^{-/-}*Mdr2*^{-/-} mice bred under MB2 condition showed reduced colonic CD4⁺ T-cell infiltration and increased Foxp3⁺ Treg-cell accumulation compared with *Il10*^{-/-} mice (figure 1I,J).

Next, we aimed to validate our observation in *Il10*^{-/-}*Mdr2*^{-/-} mice using a second model of experimental sclerosing cholangitis. To this end, we fed *Il10*^{-/-} mice a 3,5-dithioxycarbonyl-1,4-dihydrocollidine (DDC) diet.²⁷ We used mice with the more colitogenic MB2 microbiota (figure 2A). DDC diet-induced sclerosing cholangitis in *Il10*^{-/-} mice as determined by blood transaminase levels and fibrosis development (online supplemental figure S3A,B). In line with our results in *Il10*^{-/-}*Mdr2*^{-/-} mice, colitis severity and CD4⁺ T-cell infiltration in the inflamed colon of *Il10*^{-/-} mice was attenuated under the DDC diet (figure 2B), and frequencies of colonic Foxp3⁺ Treg cells were increased compared with the regular chow diet (figure 2C,D).

Thus, sclerosing cholangitis attenuates colitis severity in mouse models and is associated with an increased colonic Foxp3⁺ Treg-cell frequency.

Attenuated colitis severity in mice with sclerosing cholangitis is dependent on Foxp3⁺ Treg cells

Since the reduced colitis severity was associated with a shift of CD4⁺ T-cell infiltration towards Foxp3⁺ Treg cells, we hypothesised that Foxp3⁺ Treg cells contribute to the limitation of colonic inflammation. Foxp3⁺ Treg cells are well known for their capacity to limit intestinal inflammation and restore immune homeostasis.²⁸ Thus, to define the contribution of Foxp3⁺ Treg cells to the PSC-mediated attenuation of colitis, we used the T-cell transfer colitis model, in which Foxp3⁺ Treg cells are largely absent.²⁹ To that end, we induced colitis in lymphopenic *Rag1*^{-/-} and *Rag1*^{-/-}*Mdr2*^{-/-} mice, by transfer of naïve CD4⁺Foxp3⁻CD45Rb^{high} cells (figure 3A). As expected, *Rag1*^{-/-}*Mdr2*^{-/-} mice, but not *Rag1*^{-/-} mice developed concomitant sclerosing cholangitis (online supplemental figure S4,B). Next, we assessed colitis severity and found it not to be attenuated in *Rag1*^{-/-}*Mdr2*^{-/-} mice, but in fact to be significantly increased compared with *Rag1*^{-/-} based on weight loss and endoscopic score (figure 3B,C). As expected, no considerable Foxp3⁺ Treg-cell levels were detectable among CD4⁺ T-cell infiltrating cells (figure 3D,E).

Taken together, the protective effect of sclerosing cholangitis on colitis appears to be dependent on the presence of Foxp3⁺ Treg cells.

FMT from *Mdr2*^{-/-} mice into germ-free wild-type mice attenuates colitis severity

Alterations in the intestinal microbiota are a hallmark of IBD.³⁰ Moreover, the intestinal microbiota is known to impact Foxp3⁺ Treg-cell differentiation and expansion.³¹ We therefore hypothesised that sclerosing cholangitis may alter the intestinal microbiota, and thus, reduce colitis severity. In order to test this hypothesis, we profiled the microbiota of stool samples collected from mice suffering from colitis alone (eg, *Il10*^{-/-} mice and *Rag1*^{-/-} mice on colitis induction via transfer of CD45Rb^{high} cells) and with concomitant sclerosing cholangitis (eg, *Il10*^{-/-}*Mdr2*^{-/-} mice and *Rag1*^{-/-}*Mdr2*^{-/-} mice on colitis induction via transfer of CD45Rb^{high} cells) (online supplemental figure S5). Comparison

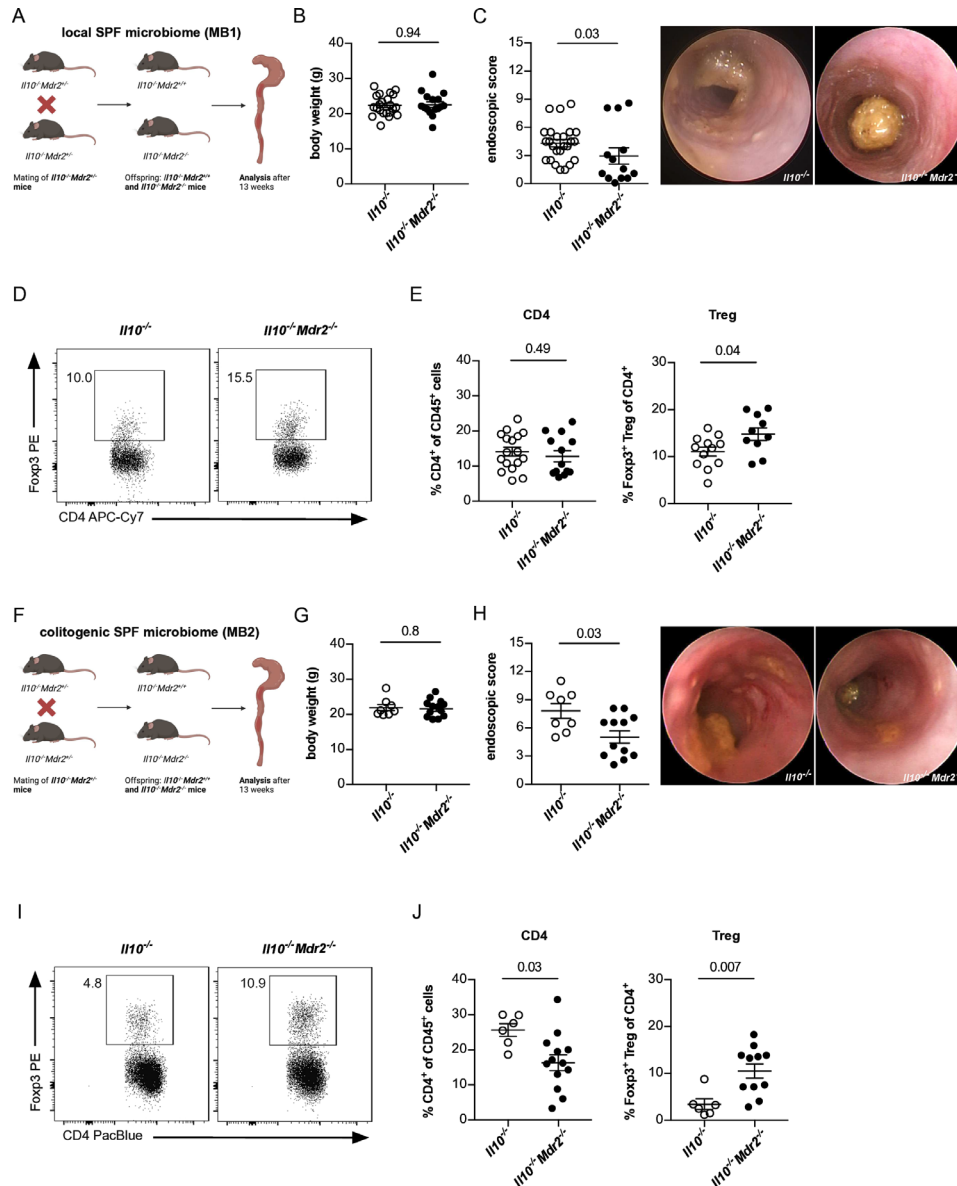


Figure 1 Spontaneous colitis is reduced in mice with concomitant experimental primary sclerosing cholangitis in $Il10^{-/-}Mdr2^{-/-}$ mice. (A) Graphical breeding scheme for generation of $Il10^{-/-}$ and $Il10^{-/-}Mdr2^{-/-}$ littermates. Mice were bred under specific pathogen-free (SPF) conditions in the local mouse facility (MB1). After weaning, litters were separated with respect to their genotype. At an age of 12 weeks, (B) body weight ($n=22$ $Il10^{-/-}$, $n=16$ $Il10^{-/-}Mdr2^{-/-}$) and (C) colon inflammation was assessed by mouse colonoscopy ($n=25$ $Il10^{-/-}$, $n=13$ $Il10^{-/-}Mdr2^{-/-}$), as described in material and methods. (D, E) Flow cytometry analysis of colon infiltrating $CD4^{+}$ T-cell ($n=17$ $Il10^{-/-}$, $n=13$ $Il10^{-/-}Mdr2^{-/-}$) and $Foxp3^{+}$ Treg-cell frequencies of 12 weeks old mice ($n=12$ $Il10^{-/-}$, $n=10$ $Il10^{-/-}Mdr2^{-/-}$). (F) Graphical breeding scheme for generation of $Il10^{-/-}$ and $Il10^{-/-}Mdr2^{-/-}$ littermates bred in the presence of a colitogenic SPF microbiome (MB2) containing *Helicobacter hepaticus*, that was transferred to the founding animals. After weaning, litters were separated with respect to their genotype. At the age of 12 weeks (G) body weight ($n=8$ $Il10^{-/-}$, $n=13$ $Il10^{-/-}Mdr2^{-/-}$), (H) colonoscopy ($n=8$ $Il10^{-/-}$, $n=12$ $Il10^{-/-}Mdr2^{-/-}$) and (I, J) frequencies of colon infiltrating $CD4^{+}$ T cells and $Foxp3^{+}$ Treg cells ($n=6$ $Il10^{-/-}$, $n=11$ $Il10^{-/-}Mdr2^{-/-}$) were analysed. For statistical analysis, Mann-Whitney U test was performed.

of beta diversities revealed clustering with some overlap of both experimental groups (online supplemental figure S5A,C), although a spread of samples between the groups was detected in both models. Of note, on the genus level, we found several taxa that significantly differed in abundance between the groups in the transfer colitis model (online supplemental figure S5D), but only one taxon in the $Il10^{-/-}$ model (online supplemental figure S5B). Most notably, an enrichment of genera of the *Lachnospiraceae* family was found in stool samples of mice suffering from colitis with concomitant liver inflammation in transfer colitis (online supplemental figure S5D).

To decipher the functional relevance of the observed PSC-induced microbiota alterations on colitis severity, we next reconstituted germ-free wild-type mice with stool derived from mice with sclerosing cholangitis ($Mdr2^{-/-}$ mice) or without sclerosing cholangitis (wild-type mice), respectively, and induced colitis in these mice using a blocking anti-IL10 α mAb³² (figure 4A). In accordance with our above-mentioned results (figure 1B,G), a mild weight loss was observed on colitis induction, that did not differ between the groups (figure 4B). However, endoscopic colitis severity was reduced in germ-free mice reconstituted with

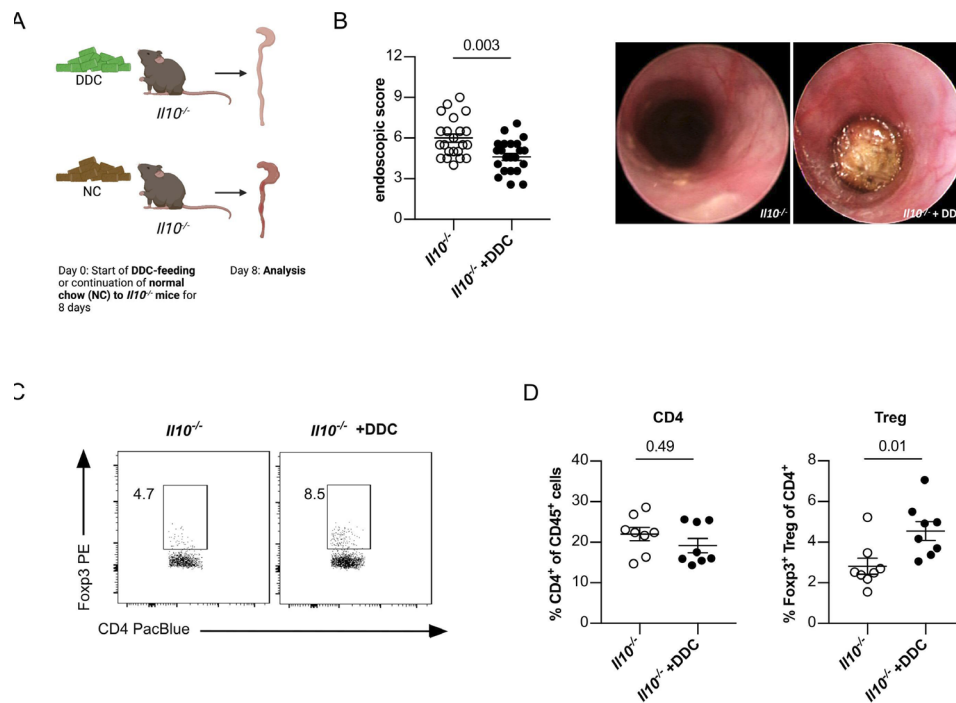


Figure 2 Spontaneous colitis is reduced in *Il10*^{-/-} mice with concomitant 3,5-diethoxycarbonyl-1,4-dihydrocollidine (DDC)-mediated liver cholestasis. (A) Graphical scheme of the experimental setup. At an age of 6–8 weeks *Il10*^{-/-} mice were gavaged with MB2. Four weeks after reconstitution, liver cholestasis was induced by 0.1% DDC feeding supplemented into the normal chow diet. After 8 days, (B) colonic inflammation was analysed by mouse colonoscopy (n=22 mice per group). (C, D) On day 9, mice were sacrificed and frequencies of colon infiltrating CD4⁺ T cells and Foxp3⁺ Treg cells were analysed using flow cytometry (8=mice per group). For statistical analysis Mann-Whitney U test was performed.

microbiota derived from *Mdr2*^{-/-} mice compared with wild-type mice (figure 4C).

Taken together, these results indicate that sclerosing cholangitis leads to alterations in the intestinal microbiota, in particular to an enrichment in genera of the *Lachnospiraceae* family. Furthermore, this altered intestinal microbiota of *Mdr2*^{-/-} mice suffering from sclerosing cholangitis is protective against colitis, when compared with wild-type mice.

Colitis severity in germ-free mice is attenuated after FMT from people with PSC-IBD compared with IBD

Based on the data obtained in the murine system, we next characterised *FOXP3* mRNA expression levels in intestinal biopsies taken from a cohort of people with CD (n=29), UC (n=22) and PSC-IBD (n=41). We observed increased *FOXP3* mRNA expression in the intestinal tissue of people with PSC-IBD compared with both, individuals with CD and UC (figure 5A). Within the cohort, we found milder IBD severity in people with concomitant PSC compared with people with CD and to a lesser extent to people with UC, as described previously (figure 5B).⁵ To account for this bias in disease severity, we next compared only those individuals with a clinically active disease as assessed by their physician. We again found an increased *FOXP3* mRNA expression in the intestinal tissue of people with PSC-IBD compared with both individuals with CD and UC (figure 5C). Of note, the mean IBD score in all three groups was low and comparable (mean IBD-score for PSC-IBD: 0.48, CD: 0.52, UC: 0.78). To further test, if this decrease is biased by biopsies from a certain location, we plotted all biopsies from the same location for all patients. We found the same trend in all locations analysed: individuals with PSC-IBD having a higher *FOXP3* mRNA expression compared with people with IBD without PSC (online supplemental figure S6A, online supplemental table S2).

Next, we measured FOXP3 protein levels in tissue sections using immunohistochemistry. To this end we focused on biopsies from the terminal ileum and sigma/rectum. In line with the mRNA expression, we found an increased number of FOXP3⁺ cells in people with PSC-IBD compared with IBD without PSC (online supplemental figure S6B,C).

Next, we aimed to test whether the microbiota from people with PSC would protect against the development of concomitant IBD. Thus, we first performed microbiota profiling of mucosa-adherent bacteria isolated from intestinal biopsies derived from our IBD and PSC-IBD cohort, that has been partially published in Wittek et al, 2023. Sequencing of faecal microbiota revealed a large overlap, but also some differences in the microbiota composition of people with IBD and those with PSC-associated IBD. However, it is important to note that our study was not powered to decipher detailed microbiota differences between PSC-IBD and IBD as this point has been addressed by previous larger studies.^{23 33} Beta diversity comparison revealed a large overlap between people with IBD and PSC-IBD (figure 6A). In fact, on the genus level only a few taxa differed in abundance between both groups (figure 6B). Interestingly, genera of the *Lachnospiraceae* family were enriched in intestinal biopsies from people with PSC-IBD compared with IBD. To test the functional relevancy of this finding, we reconstituted germ-free wild-type mice with faecal microbiota samples derived from people with IBD or PSC-IBD and induced DSS colitis on reconstitution (figure 6C). Weight loss was comparable in both groups (figure 6D). However, the colitis severity as assessed by endoscopy was significantly reduced in mice reconstituted with faecal microbiota from people with PSC-IBD compared with IBD alone (figure 6E,F). To address whether ursodeoxycholic acid (UDCA) treatment

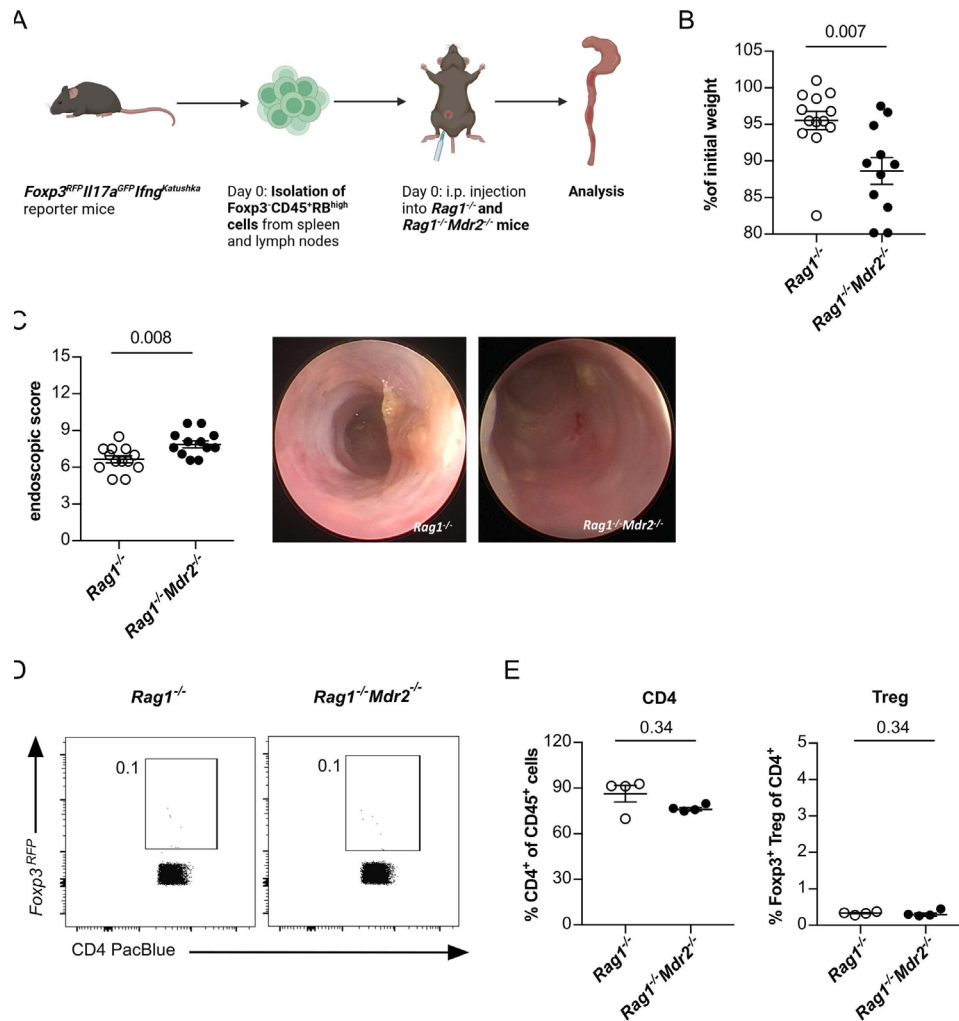


Figure 3 Increased colitis manifestation in *Rag1*^{-/-} *Mdr2*^{-/-} mice after *Foxp3*⁻ *CD45RB*^{high} T-cell transfer. (A) Graphical scheme of the experimental setup. (B) At an age of 8–10 weeks *Rag1*^{-/-} and *Rag1*^{-/-} *Mdr2*^{-/-} mice were gavaged with MB2. After 4 weeks of reconstitution, colitis was induced on transfer of flow cytometry sorted *Foxp3*⁻ *CD45RB*^{high} *CD4*⁺ T cells, isolated from *Foxp3-RFP* reporter mice. After 13 days of T-cell reconstitution, (B) weight loss and (C) colonic inflammation by colonoscopy were analysed (n=13 *Rag1*^{-/-}, n=12 *Rag1*^{-/-} *Mdr2*^{-/-}). (D, E) At day 14, mice were sacrificed and frequencies of colon infiltrating *CD4*⁺ T cells and *Foxp3*⁺ Treg cells were analysed by flow cytometry in one of three experiments (n=4 *Rag1*^{-/-}, n=4 *Rag1*^{-/-} *Mdr2*^{-/-}). For statistical analysis Mann-Whitney U test was performed.

mediates the observed effect, we performed a gnotobiotic mouse experiment. Specifically, a faecal microbiota transfer from healthy control (HC), without UDCA treatment, and primary biliary cholangitis (PBC) patients, with UDCA treatment, into germ-free mice was performed. People with PBC with mild cholestasis comparable to that of people with PSC-IBD were selected as cholestatic controls (online supplemental figure S7A,B). On engraftment, DSS-colitis was induced. A comparable colitis severity was observed between these groups, indicating that UDCA does not *per se* influence the colitis activity (online supplemental figure S7C,D). Next, we analysed whether the observed protection of these PSC-IBD-specific gnotobiotic mice is associated with an enrichment of genera of the *Lachnospiraceae* family on FMT. Microbiota profiling of donors (see online supplemental table S1 for the clinical information) and recipient mice was performed and can be found in online supplemental figure S8A. A PerMANOVA analysis showed a significant contribution of disease, group (donor vs recipient) and donor on the variation observed in the data (online supplemental figure S8B). The abundance of bacteria in the

different donors is comparable to a cross-sectional cohort (online supplemental figure S8C). When looking at the 10 highest abundant families, we observed that these were in most cases distributed similarly between recipients of the same donor, although at different proportions compared with the donor (online supplemental figure S8D). Beta diversities showed some overlapping of clusters representing each of the groups (figure 6G). Indeed, a strong enrichment of genera of the *Lachnospiraceae* family was detectable in faecal samples of mice that had been reconstituted with PSC-IBD stool compared with IBD stool (figure 6H).

In conclusion, these data indicate that PSC induces alterations of the intestinal microbiota, in particular an enrichment of genera of the *Lachnospiraceae* family, which in turn attenuate colitis susceptibility.

DISCUSSION

In line with previous reports,^{3,5} we found that people with PSC-IBD present with milder colitis severity compared with people with IBD without PSC in our cohort. Likewise, we found a lower

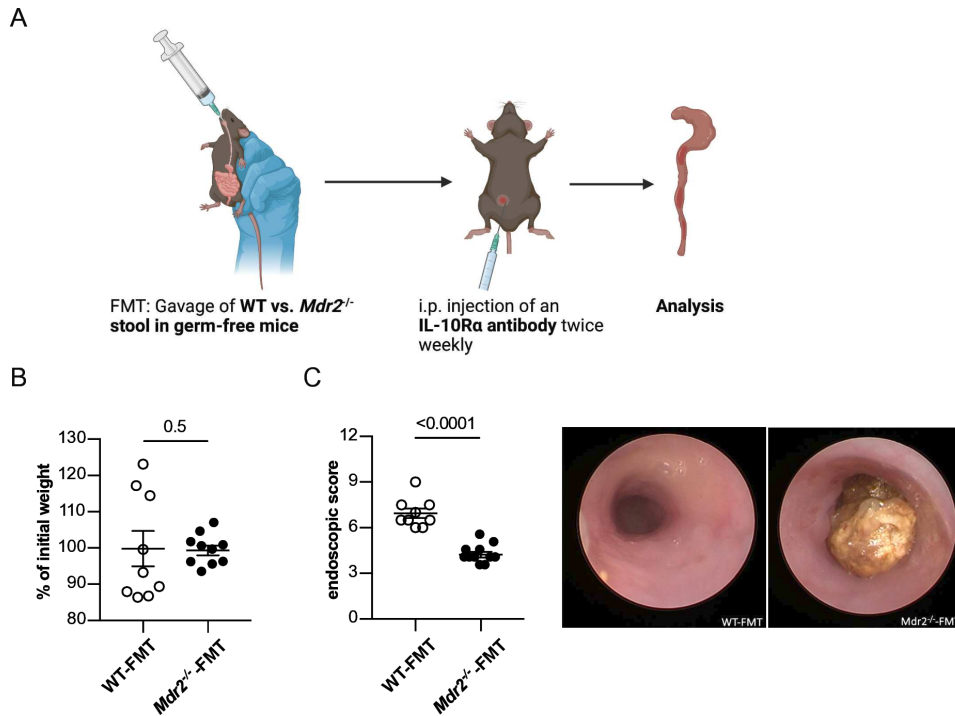


Figure 4 Reduced colitis severity in germ-free wild-type mice after transfer of *Mdr2*^{-/-} microbiota. (A) Graphical scheme of the experimental procedure. In brief, faecal microbiota obtained from wild-type and *Mdr2*^{-/-} mice, harbouring MB2 microbiome, was gavaged into germ-free wild-type mice. One day later, colitis was induced in these mice by intraperitoneal injection of 0.25 mg anti-IL10Rα antibody per mouse two times a week. After 13 days of colitis induction, (B) weight loss was determined and (C) colonic inflammation was analysed by colonoscopy (n=9 WT-FMT, n=10 *Mdr2*^{-/-}-FMT). FMT, faecal microbiota transplantation; WT, wild-type.

IBD susceptibility in a genetic (*Mdr2*^{-/-}) and an induced (DDC-diet) mouse model of sclerosing cholangitis.

Alterations in the intestinal microbiota of people with PSC-IBD and IBD without PSC have been documented in various studies. These studies have yielded somewhat divergent findings,^{19 33} possibly due to variations in participant selection criteria, sampling locations and sample processing.

Our study, along with several others, consistently identified an elevation in *Lachnospiraceae* among people with PSC-IBD compared with those with IBD without PSC.^{17 23}

It could be possible that cholestasis, which is observed in people with PSC mediates the observed effects on the intestinal microbiota. In this case a similar effect should be observed in people and mouse models with cholestasis even

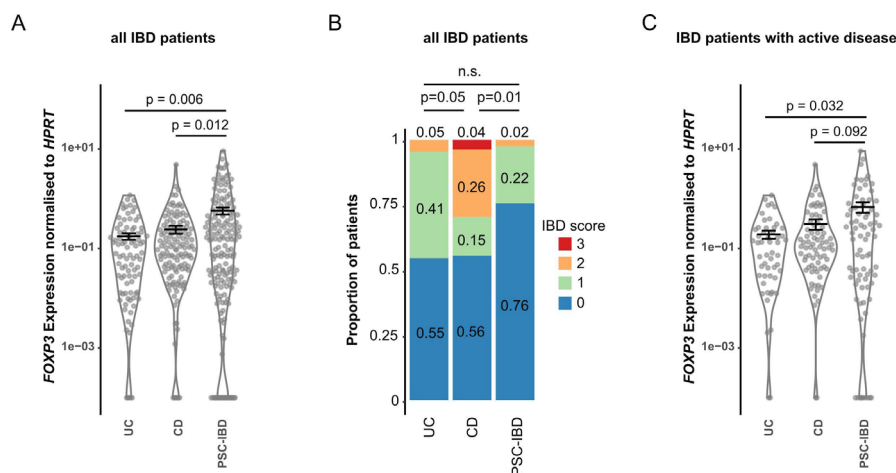


Figure 5 *FOXP3* mRNA expression and endoscopic IBD scoring reveal reduced clinical manifestation of IBD in people with primary sclerosing cholangitis (PSC-IBD). Description of a cohort including 29 people with Crohn’s disease (CD), 22 with Ulcerative colitis (UC) and 41 with PSC-IBD. (A) *FOXP3* mRNA expression levels were analysed from intestinal biopsies taken from the terminal ileum, ascending and descending colon and sigma/rectum from every person. (B) IBD severity was determined based on CDAI (persons with CD) and Mayo score (all other persons). Both scores were merged into a unified IBD score (healthy/remission: 0, mild: 1, moderate: 2, severe: 3 points). (C) *FOXP3* mRNA expression levels were analysed from intestinal biopsies taken from the terminal ileum, ascending and descending colon and sigma/rectum from every person with clinically active disease. To test for significance MLEM, post hoc Dunnett test was used for (A and C). Fisher’s exact test was used for (B).

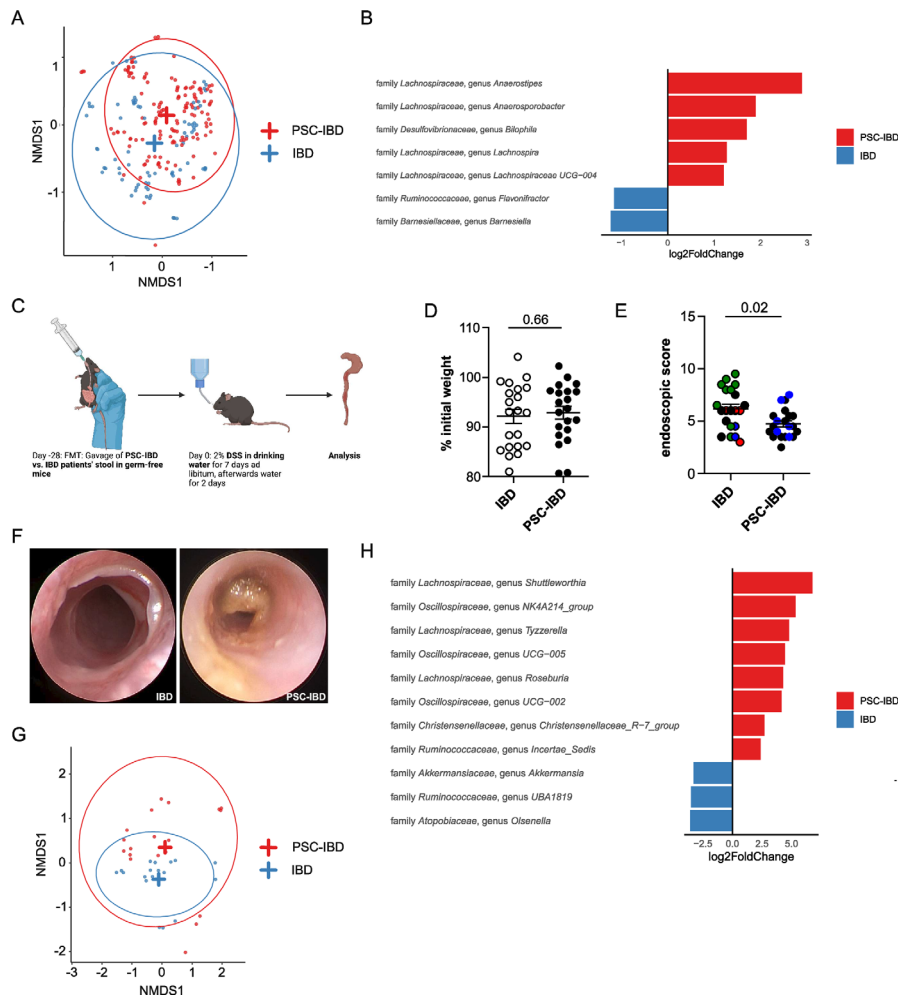


Figure 6 Colitis severity in germ-free mice is attenuated after FMT from people with primary sclerosing cholangitis and colitis (PSC-IBD), enriched for genera of the *Lachnospiraceae* family. Microbiota profiling was performed on mucosal tissue samples of our IBD and PSC-IBD cohort, as described in the material and methods. (A) PCoA of Bray-Curtis dissimilarities shows beta diversity across people with IBD and PSC-IBD. (B) Genera with significantly different abundance between people with IBD and PSC-IBD. (C) Graphical scheme of the protocol for faecal microbiota transplantation of stool derived from IBD or PSC-IBD patients into germ-free wild-type mice, and subsequent DSS colitis induction. After 9 days of colitis induction, (D) weight loss was determined and (E and F) colonic inflammation was analysed by colonoscopy (each dot represents one mouse). IBD activity of the donor is shown as: remission (black), mild (green), moderate (blue) and severe (red). (G and H) Microbiota profiling from stool samples collected from mice after reconstitution with stool samples from our IBD and PSC-IBD cohort. (D–H) $n=21$ mice transplanted with IBD stool; $n=21$ mice transplanted with PSC-IBD stool were used in four independent experiments.

in the absence of PSC. Further studies will be critical to address this point.

We observed that the protective effect of sclerosing cholangitis on colitis susceptibility was transferable on faecal microbiota transfer from *Mdr2*^{-/-} mice and people with PSC-IBD into germ-free mice. Overall, we found genera of the *Lachnospiraceae* family to be abundant in the faecal samples of people with PSC used for the faecal microbiota transfer experiment. This finding is in line with a previous study by our group.⁶ Importantly, genera of the *Lachnospiraceae* family were over-presented in faecal samples after engraftment of the germ-free mice, supporting the notion that these could be involved in the protective effect. However, there is still the limitation that the number of donors may not fully capture the range of microbiota variability in people with PSC. In line with this finding, a previous publication has reported that *Mdr2*^{-/-} mice treated with vancomycin, which reduced *Lachnospiraceae* and *Clostridiaceae*, had an increased liver pathology. Supplementation of these mice after antibiotic treatment with a 23 strain *Lachnospiraceae* consortium reduced

histological liver inflammation and fibrosis.²² Conversely, in people with PSC, the *Lachnospiraceae* *Blautia* (genus), *Lachnospiraceae* *bacterium* *1_4_56FAA* was negatively correlated with the Mayo risk score.²²

Another important observation of this study is the association between increased Foxp3⁺ Treg-cell accumulation in the colon and over-representation of *Lachnospiraceae* in faecal samples. This has been observed in our mouse models of experimental sclerosing cholangitis with concomitant colitis, and in people with PSC-IBD compared with people suffering from IBD without PSC. *Lachnospiraceae* have indeed been associated with the production of SCFAs,^{34,35} which in turn have been linked to the induction of Foxp3⁺ Treg cells.^{35–38} Therefore, further assessment of SCFAs from faecal samples of our IBD and PSC-IBD cohort and mouse models of sclerosing cholangitis is required to test whether the enrichment in *Lachnospiraceae* is indeed associated with increased SCFA levels and subsequently increased Foxp3⁺ Treg-cell numbers.

One limitation of this study is that the role of *Lachnospiraceae* remains controversial. While some taxa produce butyrate, which can strengthen the intestinal barrier, others produce propionate, which can drive mucin degradation.³⁴ More in-depth analysis of this family of bacteria in people with PSC-IBD, for example, through metagenomics, could help to identify which taxa are involved and how their metabolites could influence IBD development. Similarly, another publication³⁹ showed an increase of *Lachnospiraceae* in faecal samples of *Mdr2*^{-/-} mice. Transfer of the dysbiotic *Mdr2*^{-/-} microbiota into healthy wild-type mice induced NLRP3 activation in the gut and the liver, which sustained liver injury and promoted disease progression. It would be important to further investigate the role of different taxa of *Lachnospiraceae* in the relationship of PSC and IBD.

Interestingly, a recent study identified *Klebsiella pneumoniae* in mesenteric lymph nodes of people with PSC, and also in faecal samples.⁴⁰ Subsequent studies revealed that *K. pneumoniae* causes disruption in the epithelial barrier, resulting in the translocation of bacteria and subsequent inflammation in the liver. These discoveries emphasise how pathobionts contribute to dysfunction in the intestinal barrier and inflammation in the liver.⁴⁰ Given the crucial role of the microbiome, it would be of interest to study whether the PSC microbiota can also modify complications of IBD in PSC, such as cancer risk.

The observation that people with PSC-IBD have a lower IBD activity on average, compared with people with IBD,⁶ is also reflected in our selected donors for the faecal microbiota experiments (online supplemental table S1). However, it appears that the observed protective effect was not linked to this difference. Of note, neither *Mdr2*-deficient mice nor control mice, which were used as donors for the FMT experiment, developed spontaneous colitis. This strengthens the observation that the IBD activity of the microbiota donor on the IBD susceptibility of the recipient does not play a key role for the observed protective effect.

Another interesting question that arose during this study is whether the protective effect observed is related to the UDCA treatment that people with PSC commonly receive. Thus, we compared colitis susceptibility of germ-free wild-type mice on transfer of faecal microbiota from PBC patients, who also commonly receive UDCA, to faecal microbiota from HCs. We could not find a difference between these two groups. In addition, we transferred faecal microbiota from *Mdr2*-deficient mice, which had not received UDCA, into germ-free mice. In this set of experiments, we also observed a protective effect of the microbiota from *Mdr2*-deficient mice compared with control mice on colitis susceptibility. Therefore, our data argue against a beneficial effect of the UDCA treatment on the IBD susceptibility after FMT of PSC-IBD microbiota. However, we were not able to compare cholestatic cohorts with or without UDCA treatment and therefore, we cannot exclude an additional effect of UDCA on colitis severity mediated by the microbiota composition as it has been shown recently by He *et al.*⁴¹

Interestingly, we found an increased *FOXP3* mRNA and protein expression in the colon of people with active PSC-IBD, compared with active IBD without PSC. In addition, we identified an increased infiltration of *Foxp3*⁺ Treg cells in the inflamed colon of mice with concomitant sclerosing cholangitis in our mouse models. Interestingly, patients with genetic mutations⁴² in the *FOXP3* gene, that have no or non-functional Treg cells, develop severe intestinal inflammation. Furthermore, adoptive transfer of autologous OVA-specific or polyclonal Treg cells has been shown to reduce CD and PSC-associated UC.⁴³ Therefore, our data argue for the involvement of *Foxp3*⁺ Treg

cells in the protective effect of PSC on IBD in humans and mice. This hypothesis is supported by our finding that the protective effect of liver cholestasis on colitis severity was not detectable in the CD4⁺CD45RB^{high} T-cell transfer colitis model,^{44,45} in which *Foxp3*⁺ Treg cells are largely absent. One limitation of this experiment is that, although *Foxp3*⁺ Treg cells were depleted before the transfer into the recipient mice, there is the possibility of inducing peripheral *Foxp3*⁺ iTreg cells. However, colon infiltrating *Foxp3*⁺ Treg cells were hardly detectable in our study. Furthermore, the factors that control colonic Treg-cell accumulation during sclerosing cholangitis with concomitant colitis revealed that sclerosing cholangitis per se did not promote Treg-cell infiltration in the absence of intestinal inflammation. In fact, an increase in colonic Treg-cell accumulation was only observed in a colitogenic environment during sclerosing cholangitis. This finding is in line with a recent study by Shaw *et al* which showed that FOXP3⁺ Treg-cell frequencies gradually increase with colitis severity in intestinal biopsies of people with PSC-IBD.⁴⁶ Nevertheless, potential differences in the suppressive capabilities of colonic FOXP3⁺ Treg cells from people with IBD and PSC-IBD have not been assessed in this study and by Shaw *et al.*⁴⁶ Thus further studies will be essential to decipher the mechanism how PSC influences *Foxp3*⁺ Treg-cell expression and function in the setting of intestinal inflammation.

Overall, it remains to be elucidated what mechanism drives the increased accumulation of colonic *Foxp3*⁺ Treg cells during PSC-associated IBD. Beyond a participation of SCFAs in *Foxp3*⁺ Treg-cell differentiation in the colon, it is also tempting to speculate that the differentiation and expansion of *Foxp3*⁺ Treg cells already occurs in the cholestatic liver, and that consequently increased numbers of *Foxp3*⁺ Treg cells traffic from the liver to the colon. Indeed, increased *Foxp3*⁺ Treg-cell frequencies have been found in livers with different diseases like chronic viral hepatitis and hepatocellular carcinoma compared with healthy livers.⁴⁷ Further studies will be essential to test these hypotheses.

Interestingly, it is well known that there are shared genetic risk loci between PSC and IBD, however it is also well established that the co-occurrence is far too extensive to be explained by genetics alone.⁴⁸ Overall, our study provides novel insights into the relationship between PSC and IBD. We found that despite the common co-occurrence of both diseases, PSC can actually modify the severity of IBD to a better outcome. This effect is mediated by changes in the microbiota, which promotes the expansion of the *Foxp3*⁺ Treg-cell pool. A recently published report showed that IBD also ameliorates PSC.⁴⁹ Therefore, our data suggest that disease in one organ, for example, the liver, may modify the disease in the other, for example, the intestine, in this case limiting the disease severity in both organs. Thus, we believe that our study might serve as a basis for further investigations on the molecular mechanisms underlying these processes, and could therefore lead to the discovery of novel therapeutic targets for PSC and IBD.

Author affiliations

¹I. Department of Medicine, Section of Molecular Immunology and Gastroenterology, University Medical Center Hamburg-Eppendorf, Hamburg, Germany

²Hamburg Center for Translational Immunology (HCTI), University Medical Center Hamburg-Eppendorf, Hamburg, Germany

³Center of Diagnostics, Institute of Pathology, University Medical Center Hamburg-Eppendorf, Hamburg, Germany

⁴Institute of Pathology with the Section Molecular Pathology and Cytopathology, University Medical Center Hamburg-Eppendorf, Hamburg, Germany

⁵I. Department of Medicine, University Medical Center Hamburg-Eppendorf, Hamburg, Germany

⁶Center for Experimental Medicine, Institute of Experimental Immunology and Hepatology, University Medical Center Hamburg-Eppendorf, Hamburg, Germany

⁷Martin Zeitz Center for Rare Diseases, University Medical Center Hamburg-Eppendorf, Hamburg, Germany

Acknowledgements The authors thank Morsal Sabihi for carefully proof-reading the manuscript, and also Cathleen Haueis, Sandra Wende, Amanda Pidgornji and Saskia Domanig for technical support.

Contributors TB, FS, MT and BS collaboratively conceived, designed and carried out most of the experiments, analysed the data, provided critical intellectual input and drafted the manuscript. RJ, SB, DR and AF performed experiments and analysed data. JK provided critical intellectual input and aided in drafting the manuscript. MB and SW performed histological analysis of colon and liver pathology. ML, TC and GS performed immunohistochemistry staining of FOXP3 in human. NG, SC and GT provided critical intellectual input. TB, PP and SH collaboratively conceived and designed most experiments, supervised the study, drafted the manuscript and provided critical intellectual input. SH is acting as guarantor.

Funding This work was supported by the Deutsche Forschungsgemeinschaft (CRU306 to SH and SC (290522633 and 426581255), SFB841 to SH). SH has an endowed Heisenberg-Professorship awarded by the Deutsche Forschungsgemeinschaft.

Competing interests None declared.

Patient and public involvement Patients and/or the public were not involved in the design, or conduct, or reporting, or dissemination plans of this research.

Patient consent for publication Consent obtained directly from patient(s).

Ethics approval This study involves human participants and was approved by Ethical commission of the medical association Hamburg (PV4444, PV7106). Participants gave informed consent to participate in the study before taking part.

Provenance and peer review Not commissioned; externally peer reviewed.

Data availability statement Data are available upon reasonable request. All data relevant to the study are included in the article or uploaded as supplementary information.

Supplemental material This content has been supplied by the author(s). It has not been vetted by BMJ Publishing Group Limited (BMJ) and may not have been peer-reviewed. Any opinions or recommendations discussed are solely those of the author(s) and are not endorsed by BMJ. BMJ disclaims all liability and responsibility arising from any reliance placed on the content. Where the content includes any translated material, BMJ does not warrant the accuracy and reliability of the translations (including but not limited to local regulations, clinical guidelines, terminology, drug names and drug dosages), and is not responsible for any error and/or omissions arising from translation and adaptation or otherwise.

Open access This is an open access article distributed in accordance with the Creative Commons Attribution 4.0 Unported (CC BY 4.0) license, which permits others to copy, redistribute, remix, transform and build upon this work for any purpose, provided the original work is properly cited, a link to the licence is given, and indication of whether changes were made. See: <https://creativecommons.org/licenses/by/4.0/>.

ORCID iDs

Tanja Bedke <http://orcid.org/0000-0001-8246-1684>

Samuel Huber <http://orcid.org/0000-0001-9325-8227>

REFERENCES

- de Vries AB, Janse M, Blokzijl H, *et al*. Distinctive inflammatory bowel disease phenotype in primary sclerosing cholangitis. *World J Gastroenterol* 2015;21:1956–71.
- Rasmussen HH, Fallingborg JF, Mortensen PB, *et al*. Hepatobiliary dysfunction and primary sclerosing cholangitis in patients with Crohn's disease. *Scand J Gastroenterol* 1997;32:604–10.
- Loftus EV Jr, Harewood GC, Loftus CG, *et al*. PSC-IBD: a unique form of inflammatory bowel disease associated with primary sclerosing cholangitis. *Gut* 2005;54:91–6.
- Boonstra K, Beuers U, Ponsioen CY. Epidemiology of primary sclerosing cholangitis and primary biliary cirrhosis: a systematic review. *J Hepatol* 2012;56:1181–8.
- Weismüller TJ, Trivedi PJ, Bergquist A, *et al*. Patient age, sex, and inflammatory bowel disease phenotype associate with course of primary sclerosing cholangitis. *Gastroenterology* 2017;152:1975–84.
- Wittek A, Steglich B, Casar C, *et al*. A gradient of intestinal inflammation in primary Sclerosing cholangitis. *Inflamm Bowel Dis* 2023;izad137.
- Mohammadnia-Afrouzi M, Zavarani Hosseini A, Khalili A, *et al*. Decrease of CD4(+) CD25(+) CD127(Low) FoxP3(+) regulatory T cells with impaired suppressive function in untreated ulcerative colitis patients. *Autoimmunity* 2015;48:556–61.
- Schwinge D, von Haxthausen F, Quaa A, *et al*. Dysfunction of hepatic regulatory T cells in experimental sclerosing cholangitis is related to IL-12 signaling. *J Hepatol* 2017;66:798–805.
- Nothnagel M, Ellinghaus D, Schreiber S, *et al*. A comprehensive evaluation of SNP genotype imputation. *Hum Genet* 2009;125:163–71.
- Ellinghaus D, Jostins L, Spain SL, *et al*. Analysis of five chronic inflammatory diseases identifies 27 new associations and highlights disease-specific patterns at shared Loci. *Nat Genet* 2016;48:510–8.
- Sebedo M, Peiseler M, Franke B, *et al*. Reduced FoxP3(+) regulatory T cells in patients with primary sclerosing cholangitis are associated with IL2Ra gene Polymorphisms. *J Hepatol* 2014;60:1010–6.
- Goldberg R, Clough JN, Roberts LB, *et al*. A Crohn's disease-associated IL2Ra enhancer variant determines the balance of T cell immunity by regulating responsiveness to IL-2 signalling. *J Crohns Colitis* 2021;15:2054–65.
- Arpaia N, Campbell C, Fan X, *et al*. Metabolites produced by commensal bacteria promote peripheral regulatory T-cell generation. *Nature* 2013;504:451–5.
- Sakaguchi S, Sakaguchi N, Asano M, *et al*. Immunologic self-tolerance maintained by activated T cells expressing IL-2 receptor alpha-chains (Cd25). breakdown of a single mechanism of self-tolerance causes various autoimmune diseases. *J Immunol* 1995;155:1151–64.
- Da Cunha T, Vaziri H, Wu GY. Primary Sclerosing cholangitis and inflammatory bowel disease: a review. *J Clin Transl Hepatol* 2022;10:531–42.
- Rossen NG, Fuentes S, Boonstra K, *et al*. The mucosa-associated microbiota of PSC patients is characterized by low diversity and low abundance of uncultured clostridiales II. *J Crohns Colitis* 2015;9:342–8.
- Torres J, Bao X, Goel A, *et al*. The features of mucosa-associated microbiota in primary sclerosing cholangitis. *Aliment Pharmacol Ther* 2016;43:790–801.
- Sabino J, Vieira-Silva S, Machiels K, *et al*. Primary Sclerosing cholangitis is characterised by intestinal dysbiosis independent from IBD. *Gut* 2016;65:1681–9.
- Kummen M, Holm K, Anmarkrud JA, *et al*. The gut microbial profile in patients with primary sclerosing cholangitis is distinct from patients with ulcerative colitis without biliary disease and healthy controls. *Gut* 2017;66:611–9.
- Rühlemann MC, Heinsen F-A, Zenouzi R, *et al*. Faecal microbiota profiles as diagnostic biomarkers in primary sclerosing cholangitis. *Gut* 2017;66:753–4.
- Kevans D, Tyler AD, Holm K, *et al*. Characterization of intestinal microbiota in ulcerative colitis patients with and without primary sclerosing cholangitis. *J Crohns Colitis* 2016;10:330–7.
- Awoniyi M, Wang J, Ngo B, *et al*. Protective and aggressive bacterial subsets and metabolites modify hepatobiliary inflammation and fibrosis in a murine model of PSC. *Gut* 2023;72:671–85.
- Quraishi MN, Sergeant M, Kay G, *et al*. The gut-adherent microbiota of PSC-IBD is distinct to that of IBD. *Gut* 2017;66:386–8.
- Kühn R, Löhler J, Rennick D, *et al*. Interleukin-10-deficient mice develop chronic enterocolitis. *Cell* 1993;75:263–74.
- Fickert P, Pollheimer MJ, Beuers U, *et al*. Characterization of animal models for primary sclerosing cholangitis (PSC). *J Hepatol* 2014;60:1290–303.
- Roy U, Gálvez EJC, Iljazovic A, *et al*. Distinct microbial communities trigger colitis development upon intestinal barrier damage via innate or adaptive immune cells. *Cell Rep* 2017;21:994–1008.
- Pose E, Sancho-Bru P, Coll M. 3,5-Diethoxycarbonyl-1,4-dihydrocollidine diet: a rodent model in cholestasis research. *Methods Mol Biol* 2019;1981:249–57.
- Soukou S, Brockmann L, Bedke T, *et al*. Role of IL-10 receptor signaling in the function of CD4+ T-regulatory type 1 cells: T-cell therapy in patients with inflammatory bowel disease. *Crit Rev Immunol* 2018;38:415–31.
- Kamanaka M, Huber S, Zenewicz LA, *et al*. Memory/Effector (CD45RB(Lo)) Cd4 T cells are controlled directly by IL-10 and cause IL-22-dependent intestinal pathology. *J Exp Med* 2011;208:1027–40.
- Schirmer M, Garner A, Vlamakis H, *et al*. Microbial genes and pathways in inflammatory bowel disease. *Nat Rev Microbiol* 2019;17:497–511.
- Song X, Sun X, Oh SF, *et al*. Microbial bile acid metabolites modulate gut Rorgamma(+) regulatory T cell homeostasis. *Nature* 2020;577:410–5.
- Asseman C, Mauze S, Leach MW, *et al*. An essential role for interleukin 10 in the function of regulatory T cells that inhibit intestinal inflammation. *J Exp Med* 1999;190:995–1004.
- Rühlemann M, Liwinski T, Heinsen F-A, *et al*. Consistent alterations in faecal microbiomes of patients with primary sclerosing cholangitis independent of associated colitis. *Aliment Pharmacol Ther* 2019;50:580–9.
- Vacca M, Celano G, Calabrese FM, *et al*. The controversial role of human gut lachnospiraceae. *Microorganisms* 2020;8:573.
- Parada Venegas D, De la Fuente MK, Landskron G, *et al*. Short chain fatty acids (Scfas)-mediated gut epithelial and immune regulation and its relevance for inflammatory bowel diseases. *Front Immunol* 2019;10:277.
- Smith PM, Howitt MR, Panikov N, *et al*. The microbial metabolites, short-chain fatty acids, regulate colonic Treg cell homeostasis. *Science* 2013;341:569–73.
- Kim CH. Control of lymphocyte functions by gut microbiota-derived short-chain fatty acids. *Cell Mol Immunol* 2021;18:1161–71.
- Furusawa Y, Obata Y, Fukuda S, *et al*. Commensal microbe-derived butyrate induces the differentiation of colonic regulatory T cells. *Nature* 2013;504:446–50.

- 39 Liao L, Schneider KM, Galvez EJC, *et al.* Intestinal dysbiosis augments liver disease progression via NLRP3 in a murine model of primary Sclerosing cholangitis. *Gut* 2019;68:1477–92.
- 40 Nakamoto N, Sasaki N, Aoki R, *et al.* Gut Pathobionts underlie intestinal barrier dysfunction and liver T helper 17 cell immune response in primary sclerosing cholangitis. *Nat Microbiol* 2019;4:492–503.
- 41 He Q, Wu J, Ke J, *et al.* Therapeutic role of ursodeoxycholic acid in colitis-associated cancer via gut microbiota modulation. *Mol Ther* 2023;31:585–98.
- 42 Bacchetta R, Passerini L, Gambineri E, *et al.* Defective regulatory and effector T cell functions in patients with FoxP3 mutations. *J Clin Invest* 2006;116:1713–22.
- 43 Desreumaux P, Foussat A, Allez M, *et al.* Safety and efficacy of antigen-specific regulatory T-cell therapy for patients with refractory Crohn's disease. *Gastroenterology* 2012;143:1207–17.
- 44 Powrie F, Leach MW, Mauze S, *et al.* Phenotypically distinct subsets of CD4+ T cells induce or protect from chronic intestinal inflammation in C. B-17 Scid mice. *Int Immunol* 1993;5:1461–71.
- 45 Powrie F, Correa-Oliveira R, Mauze S, *et al.* Regulatory interactions between CD45RBhigh and CD45RBlow CD4+ T cells are important for the balance between protective and pathogenic cell-mediated immunity. *J Exp Med* 1994;179:589–600.
- 46 Shaw DG, Aguirre-Gamboa R, Vieira MC, *et al.* Antigen-driven colonic inflammation is associated with development of dysplasia in primary sclerosing cholangitis. *Nat Med* 2023;29:1520–9.
- 47 Oo YH, Weston CJ, Lalor PF, *et al.* Distinct roles for CCR4 and CXCR3 in the recruitment and positioning of regulatory T cells in the inflamed human liver. *J Immunol* 2010;184:2886–98.
- 48 Ji S-G, Juran BD, Mucha S, *et al.* Genome-wide association study of primary sclerosing cholangitis identifies new risk Loci and Quantifies the genetic relationship with inflammatory bowel disease. *Nat Genet* 2017;49:269–73.
- 49 Gui W, Hole MJ, Molinaro A, *et al.* Colitis ameliorates cholestatic liver disease via suppression of bile acid synthesis. *Nat Commun* 2023;14:3304.

1 Extended methods

2

3 Mice

4 *Rag1*^{-/-} mice, *Foxp3*^{RFP}*Ifng*^{Katushka}*Il17a*^{GFP} reporter mice, *Il10*^{-/-} mice, *Mdr2*^{-/-} mice, *Il10*^{-/-}
5 *Mdr2*^{-/-} mice, and *Rag1*^{-/-}*Mdr2*^{-/-} mice were bred and housed under specific pathogen-
6 free conditions (SPF) at the animal facility of the University Hospital Hamburg-
7 Eppendorf. *Il10*^{-/-}*Mdr2*^{+/-} were crossed with each other in order to obtain *Il10*^{-/-} and *Il10*^{-/-}
8 *Mdr2*^{-/-} littermates. These mice were then separated with respect to their genotype
9 after weaning. This way the mice could develop a specific microbiota dependent on
10 the genotype. *Il10*^{-/-}*Mdr2*^{+/-} mice were bred with two different microbiomes, one that
11 does not induce spontaneous colitis (MB1) and a colitogenic microbiome (MB2),
12 containing *Helicobacter hepaticus*(24). Littermates were separated with respect to their
13 genotype. C57BL/6 wild-type mice were bred and housed under germ-free conditions
14 at the UKE, Hamburg. All animals were housed under a 12h dark/light cycle with an
15 ambient temperature of 22°C ± 1°C and 50% ± 5% relative humidity. Food and water
16 were provided *ad libitum*. Male and female 13 ± 1 week old littermates were used for
17 all experiments. Animal experiments were approved by the local ethics committee
18 (N17/2012, N39/2021, N54/2022, N95/2023).

19

20 Human studies

21 Intestinal biopsies were taken from people undergoing colonoscopy at University
22 Hospital Hamburg-Eppendorf. We collected 2 paired biopsies at 4 sampling sites in the
23 colon and terminal ileum. One was used for RNA extraction while the other was used
24 for microbiota profiling. The biopsies were snap-frozen in liquid nitrogen directly after
25 colonoscopy and stored at -80°C until processing. For detailed patient information
26 (age, BMI, years of diagnosis, smoking, gender, IBD activity and medication) see
27 Wittek et al, 2023. Patients were included, if older than 18 years and without antibiotics
28 treatment for 6 months prior to endoscopy. Patients with infectious colitis, celiac
29 disease, or confirmed pregnancy were excluded. Disease severity was based on Mayo
30 score for UC (remission: 0-2, mild: 3-5, moderate: 6-10, severe 11-12 points) and
31 Harvey-Bradshaw index for CD (remission: 0-4, mild: 5-7, moderate: 8-16, severe >16
32 points). For comparison of IBD patients we assigned scores for disease severity
33 (remission: 0, mild: 1, moderate: 2, severe 3 points)(25). Human studies were
34 approved by the local ethical committee (Ethik Kommission der Ärztekammer Hamburg

35 PV4444, PV7106). Patients or the public were not involved in the design, or conduct,
36 or reporting, or dissemination plans of our research.

37

38 **DDC-induced sclerosing cholangitis**

39 The chemically-induced model for experimental sclerosing cholangitis, 3,5-
40 diethoxycarbonyl-1,4-dihydrocollidine (DDC; Merk, Germany) was used, by adding 0.1
41 % DDC *w/w* to the diet. *Il10*^{-/-} mice at 10–14-weeks old were fed for 8 days *ad libitum*
42 with a DDC diet. At day 8, mouse development of intestinal inflammation was assessed
43 by endoscopy. One day later, mice were sacrificed and organs were processed as
44 indicated.

45

46 **Transfer colitis**

47 Lymphocytes were isolated from the spleen and lymph nodes of
48 *Foxp3*^{RFP}*Il17a*^{Katushka}*Il10*^{GFP} reporter mice, and CD4⁺ T cells were pre-enriched using
49 MACS according to the manufacturer's instructions (Miltenyi Biotech, Bergisch-
50 Gladbach, Germany). Naïve CD4⁺ CD45RB^{high} *Foxp3*^{RFP}- T cells were fluorescence
51 activated cell sorted after incubation with anti-mouse CD4-PacBlue and CD45RB-
52 AF647 fluorochrome-labeled antibodies (both Biolegend, London, England) using
53 theAria III device (BD Biosciences, Heidelberg, Germany). To induce colitis, 2x10⁴
54 Naïve CD4⁺ CD45RB^{high} *Foxp3*^{RFP}- T cells were injected intraperitoneally into *Rag1*^{-/-}
55 and *Rag1*^{-/-}*Mdr2*^{-/-} mice. Mice were monitored for development of intestinal
56 inflammation by weight loss and endoscopy.

57

58 **Anti-IL-10 receptor antibody-induced colitis**

59 Mice were each injected with 250 µg of anti-IL10 receptor-alpha (anti-IL10Ra; clone:
60 1B1, source: HHMI, R.A. Flavell) twice a week intraperitoneally. Colitis development
61 was monitored by weight loss and endoscopy. Thirteen days after the first injection,
62 mice were sacrificed and analyzed for pathological conditions of the intestine.

63

64 **DSS colitis**

65 Mice received drinking water supplemented with 2% DSS for 7 days, followed by 2
66 days of pure drinking water in the absence of DSS, to induce acute DSS colitis (DSS
67 m.w.: 36.000–50.000; MP Biomedicals, Illkirch, France). Colitis development was

68 monitored by endoscopy. The mice were sacrificed and analyzed for pathological
69 conditions of the intestine.

70

71 **Endoscopy**

72 Colonoscopy was performed at the indicated time points to monitor the severity of
73 intestinal inflammation as described before (Becker *et al.*, 2006) using the Coloview
74 System (Karl Storz, Germany). In brief, anesthetized mice were endoscopically scored
75 concerning 5 parameters: thickening of the colon, changes in vascular pattern,
76 granularity of the mucosal surface, stool consistency, and visible fibrin, each graded 1
77 to 3, resulting in an overall score between 0 (healthy) and 15 (severe colitis).

78

79 **Fecal microbiota transplantation**

80 For murine fecal transplantation, donor mice with a colitogenic microbiome (MB2) were
81 sacrificed and stool was collected from the colon, including the caecum, directly into
82 thioglycolate medium (Merck, Darmstadt, Germany). Pooled samples from a minimum
83 of 5 mice were smashed through a 70 µm cell strainer, frozen, and stored at -80°C.
84 Upon use, stool samples were thawed, transferred to BHI medium (Merck, Darmstadt,
85 Germany), and centrifuged for 10 min at 500g. The supernatant was resuspended in
86 BHI medium and immediately gavaged. Each mouse was gavaged with 200 µl of stool.
87 For human FMT, stool samples from people with IBD and PSC-IBD, coming to the
88 clinic for routine care appointments were collected and frozen in 20% glycerol and
89 processed for transfer into germ-free mice as described above.

90

91 **Taxonomic microbiota analysis**

92 Fresh stool samples of humans and mice were collected and immediately stored at
93 -20°C until analysis. DNA was extracted according to established protocols using a
94 method combining mechanical disruption (bead-beating) and phenol/chloroform-based
95 purification previously described (Turnbaugh *et al.*, 2009). Briefly, a sample was
96 suspended in a solution containing 500 µL of extraction buffer (200 mM Tris, 20 mM
97 EDTA, and 200 mM NaCl [pH 8.0]), 200 µL of 20% SDS, 500 µL of
98 phenol:chloroform:isoamyl alcohol (24:24:1). Samples were homogenized twice with a
99 bead beater for 2 min. After precipitation of DNA, crude DNA extracts were
100 resuspended in Tris, EDTA (TE) buffer. Amplification of the V3-V4 region of the 16S

101 rRNA gene was performed according to previously described protocols. Samples were
102 sequenced on an Illumina NovaSeq platform (PE250).
103 **Microbiota** profiling of adherent microbiota of human intestinal biopsies was carried out
104 as described (Wittek *et al.*, 2023). Briefly, DNA was extracted using the DNeasy Blood
105 & Tissue Kit, followed by amplification of variable regions V1 and V2 of the 16S rRNA
106 gene. PCR products were verified and quantified before pooling and sequencing on
107 the Illumina MiSeq v3 2x300bp. Demultiplexing after sequencing was based on 0
108 mismatches in the barcode sequences. We processed both data sets with the same
109 pipeline (dada2, pyhloseq, DESeq2) and reference data base (Silva). **Where**
110 **sequencing occurred in two batches, we included the batch variable in the design**
111 **formula during DESeq2 analysis**. Importantly, in both cases we sequenced all groups
112 to be compared with the same method.

113

114 **Transaminases**

115 To monitor liver damage, aspartate aminotransferase (ASAT) and alanine
116 aminotransferase (ALAT) were analyzed in blood serum at the Institute for
117 Experimental Immunology and Hepatology (UKE, Hamburg), using an automated
118 procedure (COBAS MIRA; Roche, Basel, Switzerland).

119

120 **Cell isolation**

121 Mice were sacrificed by CO₂ and O₂ and immediately perfused with 5mL PBS via the
122 left heart ventricle. Colons were harvested, rinsed in PBS, cut into small pieces, and
123 incubated in a buffer containing 1.5% DTT (AppliChem, Darmstadt, Germany) for 20
124 min at 37°C. The resulting cell suspension, including intraepithelial cells (IEL), was
125 collected. In a second step, lamina propria cells were isolated from the remaining
126 tissue using collagenase solution containing 100U/ml collagenase (Sigma-Aldrich,
127 Taufkirchen, Germany) and 1000U/ml Dnase I (AppliChem, Darmstadt, Germany).
128 Following a 45 min incubation step at 37°C, the content was smashed through a
129 100 µm cell strainer and pooled with IELs. Tissue homogenates were washed with
130 PBS + 1% FBS at 380g and 4°C for 10 min. Leukocytes were isolated using a Percoll
131 gradient (GE Healthcare, Uppsala, Sweden). After isolation, cells were processed as
132 indicated.

133

134 **Flow Cytometry**

135 For surface staining, the cells were incubated with the following fluorochrome-
136 conjugated monoclonal antibodies: anti-CD45 (clone: 30F11), anti-CD3 (clone: 17A2),
137 anti-CD4 (clone: RM4-5), and anti-CD45RB (clone:C3 63-16A) in the presence of a
138 blocking anti-FcγR mAb (clone: 2.4G2) for 20 min at 4°C. Unless otherwise specified,
139 mAbs were purchased from Biolegend (London, England).

140 For intracellular Foxp3 expression, cell surface markers were stained as described
141 above, followed by fixation of bound antibodies with 4% formalin for 30 min and
142 permeabilization with 0.1% NP-40 for 4 min both at RT. For detection, cells were
143 incubated with the PE-conjugated Foxp3 mAb (clone: JES5-16E3, eBioscience)
144 overnight at 4°C. Cells were analyzed using a Fortessa flow cytometer (BD
145 Biosciences) and FlowJo software (Tree Star, Ashland, OR, USA).

146

147 **RNA extraction and Real-Time PCR analysis**

148 Total RNA was extracted from intestinal biopsies using Trizol Reagent (Invitrogen,
149 Waltham MA) and bead beating as previously described (Pelczar *et al.*, 2016). For
150 cDNA synthesis, we used the High-Capacity cDNA Reverse Transcription Kit
151 (Thermofisher) on 2mg of RNA per reaction, following the manufacturer's instructions.
152 For Real-time PCR (RT-PCR) analysis, TaqMan Fast Advanced Master Mix
153 (Thermofisher) was used. The following TaqMan Probes were used: *FOXP3*
154 (Hs01058534_m1) and *HPRT1* (Hs02800695_m1). Relative expression was
155 normalized to HPRT and calculated using the 2^{-DDCt} method. For significance testing,
156 we applied a linear mixed-effects model using the lme function in the nlme R package
157 (version 3.1) with the patient ID included as a random effect. This was followed by
158 post-hoc testing with Dunnett's multiple comparisons, using the glht function of the
159 multcomp R package.

160

161 **Immunohistochemistry**

162 Immunohistochemistry was performed on 5µm formalin fixed and paraffin embedded
163 sections of human colonic biopsies. Slides were deparaffinized and exposed to heat-
164 induced antigen retrieval for 5 minutes in an autoclave at 121°C in pH 7.8 wash buffer
165 (Dako, Glostrup, Denmark) and primary antibody specific for FOXP3 (dilution 1:72)
166 was applied. Bound antibody was then visualized using the EnVision Kit (Dako). All
167 sections were counterstained with hematoxylin. FOXP3⁺ cells were counted in a

168 blinded fashion from at least 5 areas of a given histological section and divided by the
169 total tissue surface obtained from the 5 areas.

170

171

172 **Microbiota data analysis**

173 16S sequencing reads from mouse stool samples were processed, aligned, and
174 quantified to the level of amplicon sequence variants (ASVs) using the dada2 (version
175 1.12.1) pipeline for paired reads (Callahan *et al.*, 2016). Forward and reverse reads
176 were trimmed to 220bp. Trimmed reads with more than 2 expected errors were
177 discarded. After merging forward and reverse reads, chimera removal was performed.
178 We kept all ASVs that were observed in at least 1% of all samples. Taxonomic
179 assignment up to the genus level was performed using the SILVA database from
180 September 2019 (v138) (Quast *et al.*, 2012).

181 Further analysis of ASV count tables was carried out using phyloseq (version 1.28.0)
182 (McMurdie *et al.*, 2013). For beta diversity plots, non-metric multidimensional scaling
183 (NMDS) was applied using Bray-Curtis dissimilarity. To find differentially abundant
184 ASVs between groups, DESeq2 (version 1.36) (Love *et al.*, 2014) was used using Wald
185 statistics and parametric fitting of dispersions, followed by log₂ fold change shrinkage,
186 and adjustment for multiple testing. ASVs were then filtered to an adjusted p-value <
187 0.05, an absolute log₂ fold change > 1, and being detected in at least 3 samples.

188 **Microbiota** profiling of adherent microbiota of human intestinal biopsies was carried out
189 as described in detail in Wittek *et al.*, 2023 following a similar pipeline as for the mouse
190 stool samples. Importantly, reads from individual ASVs were pooled on the genus level
191 to account for the reduced abundance of reads obtained from biopsies compared to
192 stool.

193

194 **Statistical analysis**

195 For detailed statistical analysis of **microbiota** data, see **microbiota** data analysis above.
196 Statistical analysis of all other data was performed with the GraphPad Prism® Software
197 (GraphPad Software, San Diego, CA, USA). Non-parametric two-sided Mann–Whitney
198 test was used. The significance level alpha was set to 0.05.

199

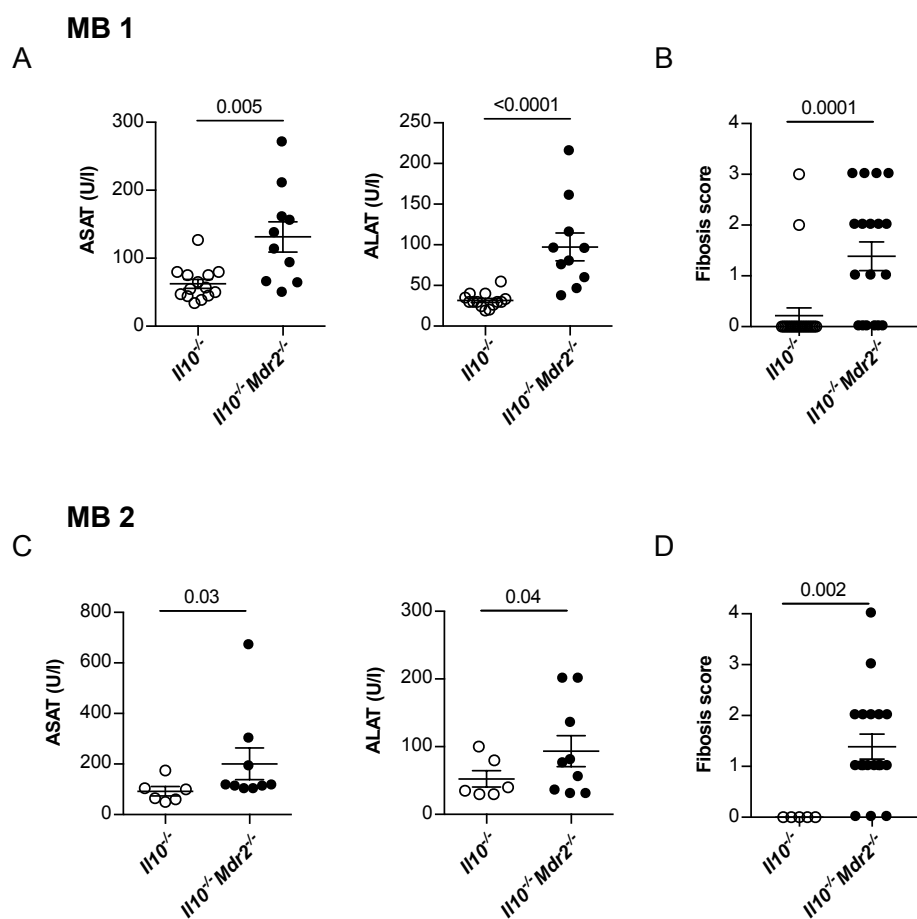


Figure S1: Liver inflammation in *Il10*^{-/-} mice with concomitant *Mdr2*^{-/-} induced cholangitis. Mice were bred under SPF conditions of the local mouse facility (MB1), as outlined in Figure 1. At 12 weeks of age, mice were sacrificed and liver pathology was assessed by (A) serum Aspartate Aminotransferase (ASAT) and Alanine Aminotransferase (ALAT) (n=14 *Il10*^{-/-}, n=10 *Il10*^{-/-}*Mdr2*^{-/-}), as described in the material and methods. (B) Fibrosis score was analyzed by Sirius Red staining. (C) Mice bred in the presence of colitogenic MB2, were sacrificed and liver pathology was analyzed based on serum Aspartate Aminotransferase (ASAT) and Alanine Aminotransferase (ALAT) (n=6 *Il10*^{-/-}, n=9 *Il10*^{-/-}*Mdr2*^{-/-}). (D) Fibrosis score was analyzed by Sirius Red staining. In all experiments, Mann-Whitney U test was performed for statistical analysis.

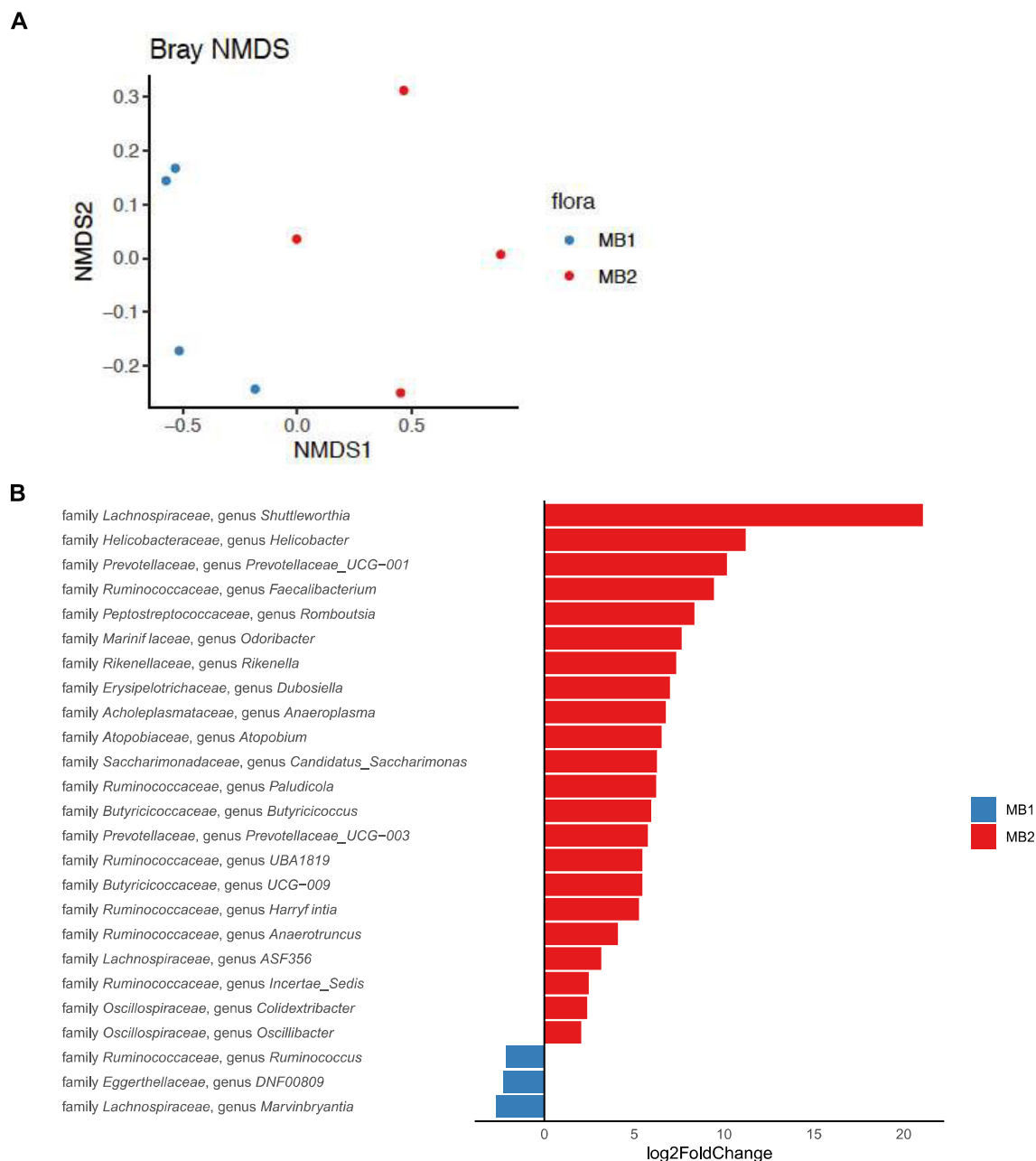


Figure S2: Microbiota profiling of MB1 and in colitogenic MB2. Wild-type mice bred under microbiota conditions 1 (MB1) and 2 (MB2) were sacrificed and stool samples from 4 mice were collected per group. Microbiota profiling was performed as described in the materials and methods. (A) PCoA of Bray-Curtis dissimilarities shows beta diversity across mice bred under MB1 and MB2 conditions. (B) Genera with significantly different abundance between groups.

Figure S2

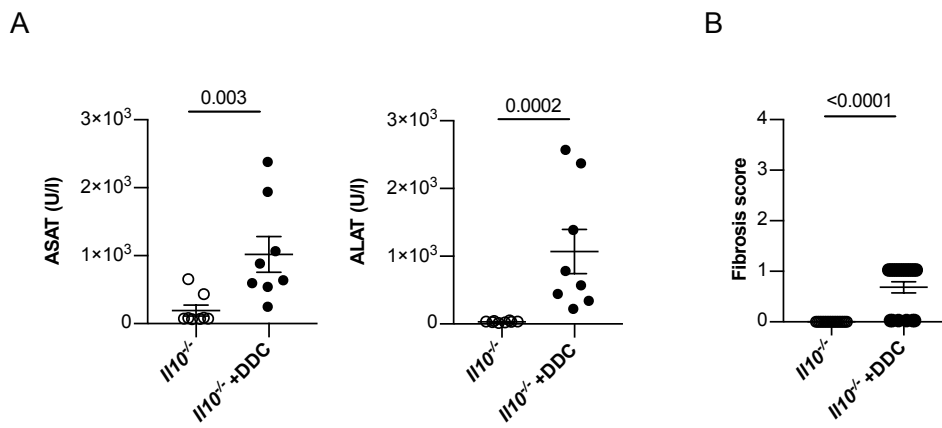


Figure S3: Liver inflammation in *Il10*^{-/-} mice after DDC-induced liver cholestasis. Liver cholestasis was induced by 2% DDC feeding in *Il10*^{-/-} mice gavaged with MB2, as described in Figure 2. After 9 days of feeding the mice with the DDC diet, mice were sacrificed and liver inflammation was analyzed by (A) serum Aspartate Aminotransferase (ASAT) and Alanine Aminotransferase (ALAT) (8= mice per group). (B) Fibrosis score was analyzed by Sirius Red staining. For statistical analysis, Mann-Whitney U test was performed.

Figure S3

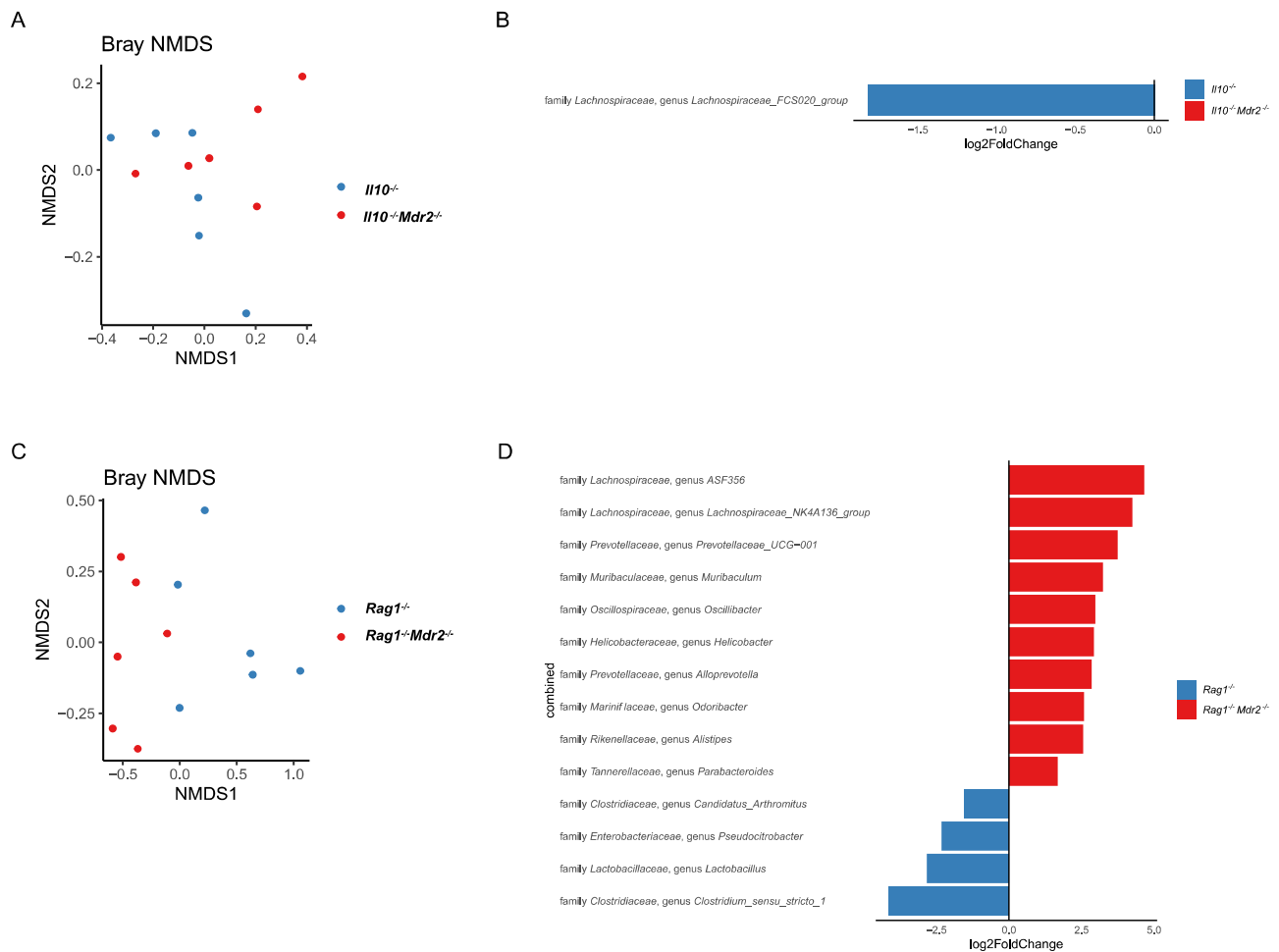


Figure S5: Concomitant liver inflammation alters the intestinal microbiota in *Il10*^{-/-} and *Rag1*^{-/-} mice suffering from colitis. *Il10*^{-/-}, *Il10*^{-/-}*Mdr2*^{-/-} mice (MB1) and *Rag1*^{-/-}, *Rag1*^{-/-}*Mdr2*^{-/-} mice (MB2) were sacrificed as described in Figures 1 and 3, respectively, and stool samples from 6 mice were collected per group. Microbiota profiling was performed as described in the materials and methods. (A) PCoA of Bray-Curtis dissimilarities shows beta diversity across *Il10*^{-/-} and *Il10*^{-/-}*Mdr2*^{-/-} mice. (B) Genera with significantly different abundances between groups. (C) PCoA of Bray-Curtis dissimilarities shows beta diversity across *Rag1*^{-/-} and *Rag1*^{-/-}*Mdr2*^{-/-} mice. (D) Genera with significantly different abundances between both groups.

Figure S5

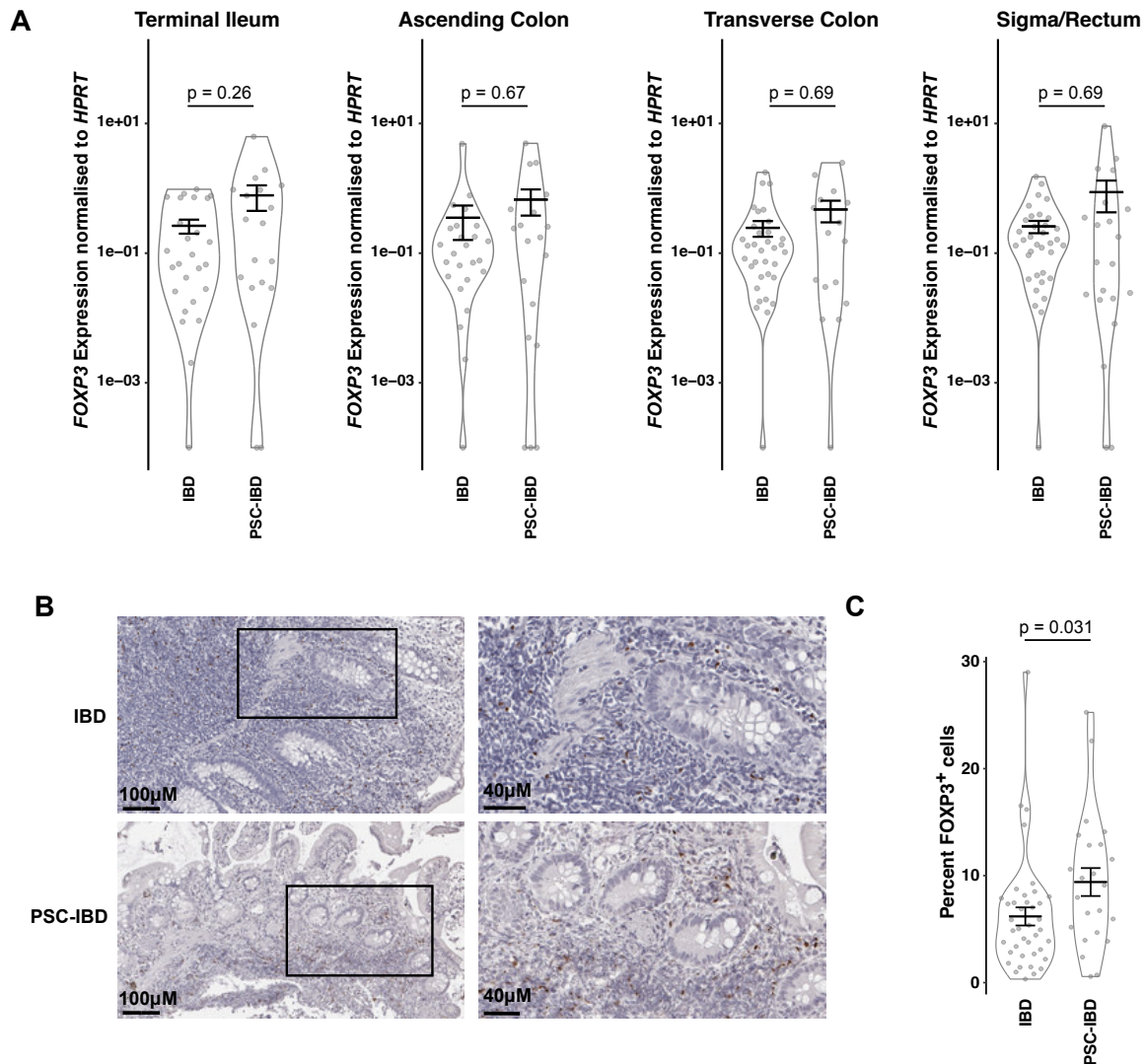


Figure S6: Increased FOXP3 protein expression in intestinal biopsies of people with PSC-IBD. (A) *FOXP3* mRNA expression levels were analyzed from intestinal biopsies taken from the terminal ileum, ascending colon, descending colon or sigma/rectum from every person with clinically active disease. (B) Representative images and (C) quantification of FOXP3⁺ cells in intestinal biopsies taken from the terminal ileum and sigma/rectum from every person with clinically active disease. To test for significance MLEM, post hoc Dunnett test was used.

Figure S6

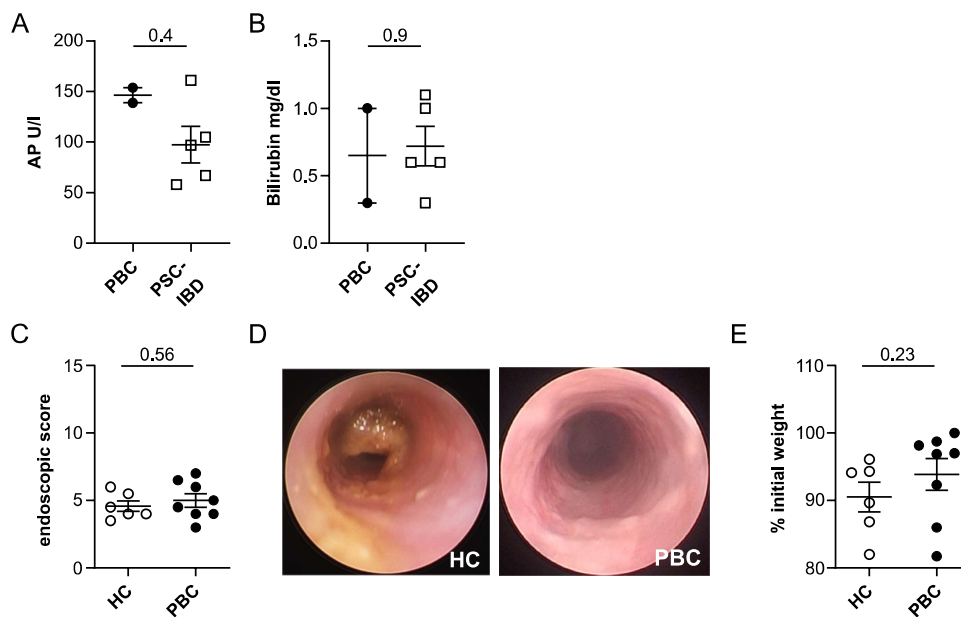


Figure S7: Colitis severity in germ-free mice is not affected by UDCA treatment of the stool donor. (A+B) People with PBC with comparable cholestasis to people with PSC-IBD were chosen. Stool transfer from healthy control (HC) and people with primary biliary cholangitis (PBC) that received UDCA treatment into germ-free mice before the chemical induction of colitis for 7 days. On day 9, colonic inflammation was analyzed by (C+D) colonoscopy as represented by endoscopic score and representative pictures and (E) weight loss. Each dot represents one mouse. For statistical analysis Mann-Whitney U test was performed.

Figure S7

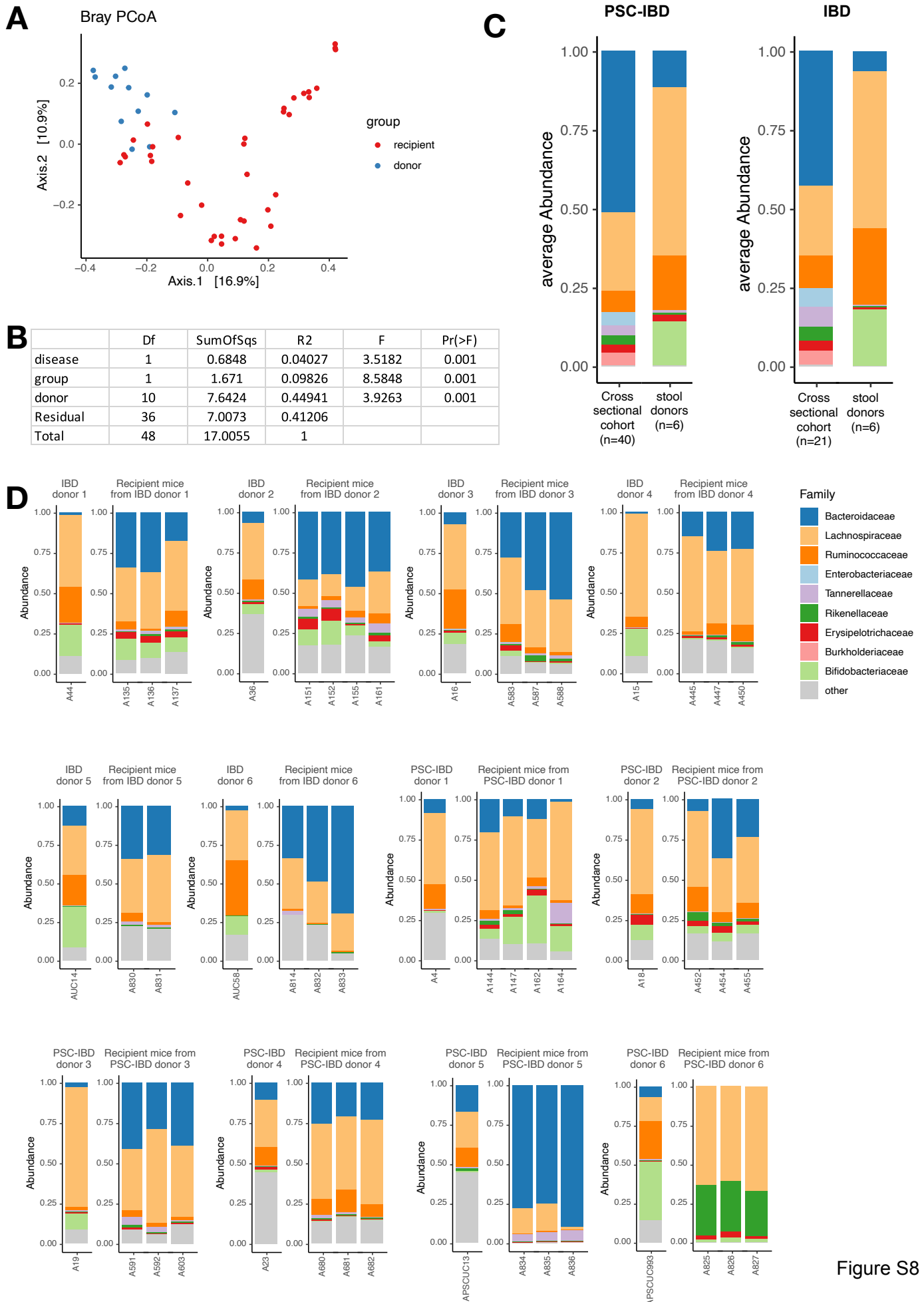


Figure S8

Figure S8: Microbiota profiling of stool from human donors and respective recipient mice. (A) PCoA of Bray-Curtis dissimilarities shows beta diversity across stool samples from human donors and recipient mice. (B) PERMANOVA analysis showing the contribution of disease, group (donor vs. recipient) and donor to the variation observed in the data shown in A. (C) A bar plot displaying the most abundant families, comparing a cross-section with the stool donors used in this study. (D) Abundance of the 10 highest abundant families across donor samples and their respective recipient mouse samples.

Table S1. Characteristics of microbiota donors.

	IBD	PSC-IBD	PBC
n-value	6	5	2
age in years	41±15.2	43±9.7	65±2.2
sex male (%)	4 (66%)	3 (60%)	2 (100%)
IBD disease activity, n (%)			
Remission	2 (33%)	3 (60%)	0 (0%)
Mild	2 (33%)	0 (0%)	0 (0%)
Moderate	1 (16%)	2 (40%)	0 (0%)
Severe	1 (16%)	0 (0%)	0 (0%)
Medications, n (%)			
5-ASA	4 (66%)	3 (60%)	0 (0%)
Thiopurines	2 (33%)	1 (20%)	0 (0%)
Anti-TNF	1 (16%)	2 (40%)	0 (0%)
Anti-IL12/23	1 (16%)	0 (0%)	0 (0%)
UDCA	0	5/5 (100%)	2/2 (100%)
Methotrexate	1 (16%)	0 (0%)	0 (0%)

*IBD disease activity was categorized based on Mayo score for UC (remission: 0-2, mild: 3-5, moderate: 6-10, severe 11-12 points).

Table S2. Characteristics of patients analyzed by immunohistochemistry

	IBD	PSC-IBD
n-value	30	19
age in years	42 ± 14.5	37 ± 14.5
sex male %	60%	84%
Disease activity, n (%)		
Remission	12 (40%)	9 (47%)
Mild	13 (43%)	7 (37%)
Moderate	3 (10%)	3 (16%)
Severe	2 (7%)	0
Medications, n (%)		
5-ASA	17 (57%)	6 (32%)
Thiopurines	2 (7%)	7 (37%)
Anti-TNF	14 (47%)	5 (26%)
Anti-IL12/23	1 (3%)	2 (11%)
UDCA	0	16 (84%)
Methotrexate	1 (3%)	0

Extended methods

Mice

Rag1^{-/-} mice, *Foxp3*^{RFP}*Ifng*^{Katushka}*Il17a*^{GFP} reporter mice, *Il10*^{-/-} mice, *Mdr2*^{-/-} mice, *Il10*^{-/-} *Mdr2*^{-/-} mice, and *Rag1*^{-/-} *Mdr2*^{-/-} mice were bred and housed under specific pathogen-free conditions (SPF) at the animal facility of the University Hospital Hamburg-Eppendorf. *Il10*^{-/-} *Mdr2*^{+/-} were crossed with each other in order to obtain *Il10*^{-/-} and *Il10*^{-/-} *Mdr2*^{-/-} littermates. These mice were then separated with respect to their genotype after weaning. This way the mice could develop a specific microbiota dependent on the genotype. *Il10*^{-/-} *Mdr2*^{+/-} mice were bred with two different microbiomes, one that does not induce spontaneous colitis (MB1) and a colitogenic microbiome (MB2), containing *Helicobacter hepaticus*(24). Littermates were separated with respect to their genotype. C57BL/6 wild-type mice were bred and housed under germ-free conditions at the UKE, Hamburg. All animals were housed under a 12h dark/light cycle with an ambient temperature of 22°C ± 1°C and 50% ± 5% relative humidity. Food and water were provided *ad libitum*. Male and female 13 ± 1 week old littermates were used for all experiments. Animal experiments were approved by the local ethics committee (N17/2012, N39/2021, N54/2022, N95/2023).

Human studies

Intestinal biopsies were taken from people undergoing colonoscopy at University Hospital Hamburg-Eppendorf. We collected 2 paired biopsies at 4 sampling sites in the colon and terminal ileum. One was used for RNA extraction while the other was used for microbiota profiling. The biopsies were snap-frozen in liquid nitrogen directly after colonoscopy and stored at -80°C until processing. For detailed patient information (age, BMI, years of diagnosis, smoking, gender, IBD activity and medication) see Wittek et al, 2023. Patients were included, if older than 18 years and without antibiotics treatment for 6 months prior to endoscopy. Patients with infectious colitis, celiac disease, or confirmed pregnancy were excluded. Disease severity was based on Mayo score for UC (remission: 0-2, mild: 3-5, moderate: 6-10, severe 11-12 points) and Harvey-Bradshaw index for CD (remission: 0-4, mild: 5-7, moderate: 8-16, severe >16 points). For comparison of IBD patients we assigned scores for disease severity (remission: 0, mild: 1, moderate: 2, severe 3 points)(25). Human studies were approved by the local ethical committee (Ethik Kommission der Ärztekammer Hamburg

PV4444, PV7106). Patients or the public were not involved in the design, or conduct, or reporting, or dissemination plans of our research.

DDC-induced sclerosing cholangitis

The chemically-induced model for experimental sclerosing cholangitis, 3,5-diethoxycarbonyl-1,4-dihydrocollidine (DDC; Merk, Germany) was used, by adding 0.1 % DDC *w/w* to the diet. *Il10*^{-/-} mice at 10–14-weeks old were fed for 8 days *ad libitum* with a DDC diet. At day 8, mouse development of intestinal inflammation was assessed by endoscopy. One day later, mice were sacrificed and organs were processed as indicated.

Transfer colitis

Lymphocytes were isolated from the spleen and lymph nodes of *Foxp3^{RFP}Il17a^{Katushka}Il10^{GFP}* reporter mice, and CD4⁺ T cells were pre-enriched using MACS according to the manufacturer's instructions (Miltenyi Biotech, Bergisch-Gladbach, Germany). Naïve CD4⁺ CD45RB^{high} *Foxp3^{RFP}*- T cells were fluorescence activated cell sorted after incubation with anti-mouse CD4-PacBlue and CD45RB-AF647 fluorochrome-labeled antibodies (both Biolegend, London, England) using the Aria III device (BD Biosciences, Heidelberg, Germany). To induce colitis, 2x10⁴ Naïve CD4⁺ CD45RB^{high} *Foxp3^{RFP}*- T cells were injected intraperitoneally into *Rag1*^{-/-} and *Rag1*^{-/-}*Mdr2*^{-/-} mice. Mice were monitored for development of intestinal inflammation by weight loss and endoscopy.

Anti-IL-10 receptor antibody-induced colitis

Mice were each injected with 250 µg of anti-IL10 receptor-alpha (anti-IL10Ra; clone: 1B1, source: HHMI, R.A. Flavell) twice a week intraperitoneally. Colitis development was monitored by weight loss and endoscopy. Thirteen days after the first injection, mice were sacrificed and analyzed for pathological conditions of the intestine.

DSS colitis

Mice received drinking water supplemented with 2% DSS for 7 days, followed by 2 days of pure drinking water in the absence of DSS, to induce acute DSS colitis (DSS m.w.: 36.000–50.000; MP Biomedicals, Illkirch, France). Colitis development was

monitored by endoscopy. The mice were sacrificed and analyzed for pathological conditions of the intestine.

Endoscopy

Colonoscopy was performed at the indicated time points to monitor the severity of intestinal inflammation as described before (Becker *et al.*, 2006) using the Coloview System (Karl Storz, Germany). In brief, anesthetized mice were endoscopically scored concerning 5 parameters: thickening of the colon, changes in vascular pattern, granularity of the mucosal surface, stool consistency, and visible fibrin, each graded 1 to 3, resulting in an overall score between 0 (healthy) and 15 (severe colitis).

Fecal microbiota transplantation

For murine fecal transplantation, donor mice with a colitogenic microbiome (MB2) were sacrificed and stool was collected from the colon, including the caecum, directly into thioglycolate medium (Merck, Darmstadt, Germany). Pooled samples from a minimum of 5 mice were smashed through a 70 µm cell strainer, frozen, and stored at -80°C. Upon use, stool samples were thawed, transferred to BHI medium (Merck, Darmstadt, Germany), and centrifuged for 10 min at 500g. The supernatant was resuspended in BHI medium and immediately gavaged. Each mouse was gavaged with 200 µl of stool. For human FMT, stool samples from people with IBD and PSC-IBD, coming to the clinic for routine care appointments were collected and frozen in 20% glycerol and processed for transfer into germ-free mice as described above.

Taxonomic microbiota analysis

Fresh stool samples of humans and mice were collected and immediately stored at -20°C until analysis. DNA was extracted according to established protocols using a method combining mechanical disruption (bead-beating) and phenol/chloroform-based purification previously described (Turnbaugh *et al.*, 2009). Briefly, a sample was suspended in a solution containing 500 µL of extraction buffer (200 mM Tris, 20 mM EDTA, and 200 mM NaCl [pH 8.0]), 200 µL of 20% SDS, 500 µL of phenol:chloroform:isoamyl alcohol (24:24:1). Samples were homogenized twice with a bead beater for 2 min. After precipitation of DNA, crude DNA extracts were resuspended in Tris, EDTA (TE) buffer. Amplification of the V3-V4 region of the 16S

rRNA gene was performed according to previously described protocols. Samples were sequenced on an Illumina NovaSeq platform (PE250).

Microbiota profiling of adherent microbiota of human intestinal biopsies was carried out as described (Wittek *et al.*, 2023). Briefly, DNA was extracted using the DNeasy Blood & Tissue Kit, followed by amplification of variable regions V1 and V2 of the 16S rRNA gene. PCR products were verified and quantified before pooling and sequencing on the Illumina MiSeq v3 2x300bp. Demultiplexing after sequencing was based on 0 mismatches in the barcode sequences. We processed both data sets with the same pipeline (dada2, pyhloseq, DESeq2) and reference data base (Silva). Where sequencing occurred in two batches, we included the batch variable in the design formula during DESeq2 analysis. Importantly, in both cases we sequenced all groups to be compared with the same method.

Transaminases

To monitor liver damage, aspartate aminotransferase (ASAT) and alanine aminotransferase (ALAT) were analyzed in blood serum at the Institute for Experimental Immunology and Hepatology (UKE, Hamburg), using an automated procedure (COBAS MIRA; Roche, Basel, Switzerland).

Cell isolation

Mice were sacrificed by CO₂ and O₂ and immediately perfused with 5mL PBS via the left heart ventricle. Colons were harvested, rinsed in PBS, cut into small pieces, and incubated in a buffer containing 1.5% DTT (AppliChem, Darmstadt, Germany) for 20 min at 37°C. The resulting cell suspension, including intraepithelial cells (IEL), was collected. In a second step, lamina propria cells were isolated from the remaining tissue using collagenase solution containing 100U/ml collagenase (Sigma-Aldrich, Taufkirchen, Germany) and 1000U/ml Dnase I (AppliChem, Darmstadt, Germany). Following a 45 min incubation step at 37°C, the content was smashed through a 100 µm cell strainer and pooled with IELs. Tissue homogenates were washed with PBS + 1% FBS at 380g and 4°C for 10 min. Leukocytes were isolated using a Percoll gradient (GE Healthcare, Uppsala, Sweden). After isolation, cells were processed as indicated.

Flow Cytometry

For surface staining, the cells were incubated with the following fluorochrome-conjugated monoclonal antibodies: anti-CD45 (clone: 30F11), anti-CD3 (clone: 17A2), anti-CD4 (clone: RM4-5), and anti-CD45RB (clone: C3 63-16A) in the presence of a blocking anti-FcγR mAb (clone: 2.4G2) for 20 min at 4°C. Unless otherwise specified, mAbs were purchased from Biolegend (London, England).

For intracellular Foxp3 expression, cell surface markers were stained as described above, followed by fixation of bound antibodies with 4% formalin for 30 min and permeabilization with 0.1% NP-40 for 4 min both at RT. For detection, cells were incubated with the PE-conjugated Foxp3 mAb (clone: JES5-16E3, eBioscience) overnight at 4°C. Cells were analyzed using a Fortessa flow cytometer (BD Biosciences) and FlowJo software (Tree Star, Ashland, OR, USA).

RNA extraction and Real-Time PCR analysis

Total RNA was extracted from intestinal biopsies using Trizol Reagent (Invitrogen, Waltham MA) and bead beating as previously described (Pelczar *et al.*, 2016). For cDNA synthesis, we used the High-Capacity cDNA Reverse Transcription Kit (ThermoFisher) on 2mg of RNA per reaction, following the manufacturer's instructions. For Real-time PCR (RT-PCR) analysis, TaqMan Fast Advanced Master Mix (ThermoFisher) was used. The following TaqMan Probes were used: *FOXP3* (Hs01058534_m1) and *HPRT1* (Hs02800695_m1). Relative expression was normalized to HPRT and calculated using the $2^{-\text{DDCt}}$ method. For significance testing, we applied a linear mixed-effects model using the lme function in the nlme R package (version 3.1) with the patient ID included as a random effect. This was followed by post-hoc testing with Dunnett's multiple comparisons, using the glht function of the multcomp R package.

Immunohistochemistry

Immunohistochemistry was performed on 5µm formalin fixed and paraffin embedded sections of human colonic biopsies. Slides were deparaffinized and exposed to heat-induced antigen retrieval for 5 minutes in an autoclave at 121°C in pH 7.8 wash buffer (Dako, Glostrup, Denmark) and primary antibody specific for FOXP3 (dilution 1:72) was applied. Bound antibody was then visualized using the EnVision Kit (Dako). All sections were counterstained with hematoxylin. FOXP3⁺ cells were counted in a

blinded fashion from at least 5 areas of a given histological section and divided by the total tissue surface obtained from the 5 areas.

Microbiota data analysis

16S sequencing reads from mouse stool samples were processed, aligned, and quantified to the level of amplicon sequence variants (ASVs) using the dada2 (version 1.12.1) pipeline for paired reads (Callahan *et al.*, 2016). Forward and reverse reads were trimmed to 220bp. Trimmed reads with more than 2 expected errors were discarded. After merging forward and reverse reads, chimera removal was performed. We kept all ASVs that were observed in at least 1% of all samples. Taxonomic assignment up to the genus level was performed using the SILVA database from September 2019 (v138) (Quast *et al.*, 2012).

Further analysis of ASV count tables was carried out using phyloseq (version 1.28.0) (McMurdie *et al.*, 2013). For beta diversity plots, non-metric multidimensional scaling (NMDS) was applied using Bray-Curtis dissimilarity. To find differentially abundant ASVs between groups, DESeq2 (version 1.36) (Love *et al.*, 2014) was used using Wald statistics and parametric fitting of dispersions, followed by log₂ fold change shrinkage, and adjustment for multiple testing. ASVs were then filtered to an adjusted p-value < 0.05, an absolute log₂ fold change > 1, and being detected in at least 3 samples.

Microbiota profiling of adherent microbiota of human intestinal biopsies was carried out as described in detail in Wittek *et al.*, 2023 following a similar pipeline as for the mouse stool samples. Importantly, reads from individual ASVs were pooled on the genus level to account for the reduced abundance of reads obtained from biopsies compared to stool.

Statistical analysis

For detailed statistical analysis of microbiota data, see microbiota data analysis above. Statistical analysis of all other data was performed with the GraphPad Prism® Software (GraphPad Software, San Diego, CA, USA). Non-parametric two-sided Mann–Whitney test was used. The significance level alpha was set to 0.05.

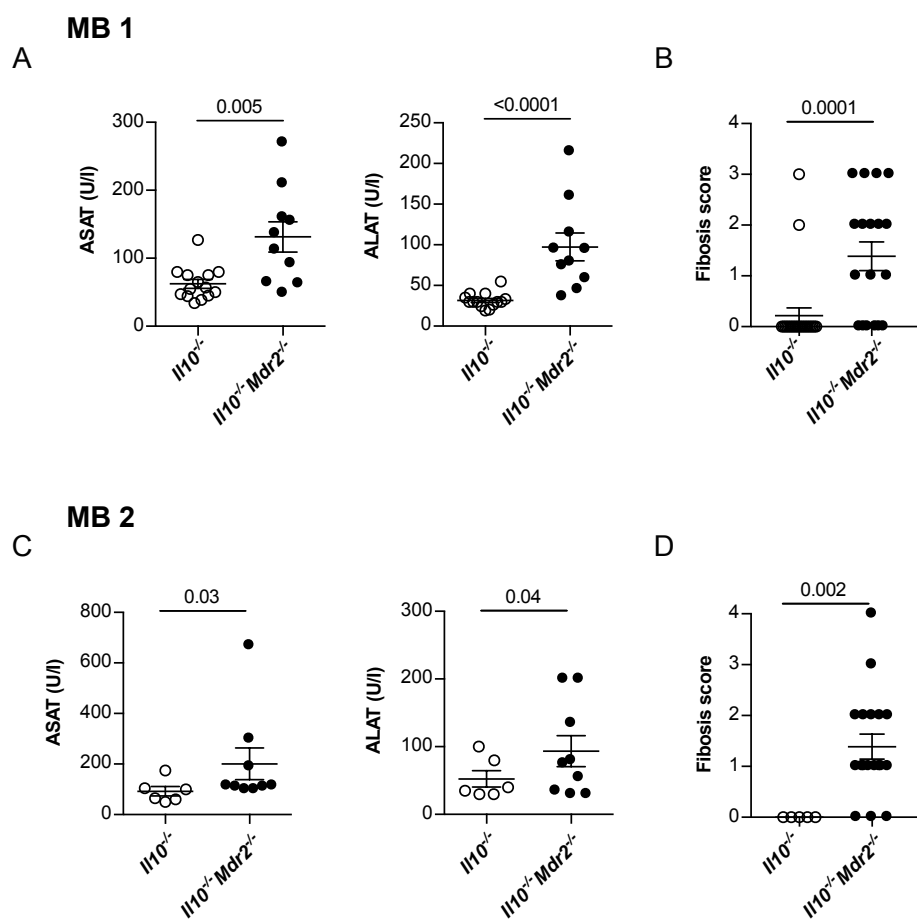


Figure S1: Liver inflammation in *Il10*^{-/-} mice with concomitant *Mdr2*^{-/-} induced cholangitis. Mice were bred under SPF conditions of the local mouse facility (MB1), as outlined in Figure 1. At 12 weeks of age, mice were sacrificed and liver pathology was assessed by (A) serum Aspartate Aminotransferase (ASAT) and Alanine Aminotransferase (ALAT) (n=14 *Il10*^{-/-}, n=10 *Il10*^{-/-}*Mdr2*^{-/-}), as described in the material and methods. (B) Fibrosis score was analyzed by Sirius Red staining. (C) Mice bred in the presence of colitogenic MB2, were sacrificed and liver pathology was analyzed based on serum Aspartate Aminotransferase (ASAT) and Alanine Aminotransferase (ALAT) (n=6 *Il10*^{-/-}, n=9 *Il10*^{-/-}*Mdr2*^{-/-}). (D) Fibrosis score was analyzed by Sirius Red staining. In all experiments, Mann-Whitney U test was performed for statistical analysis.

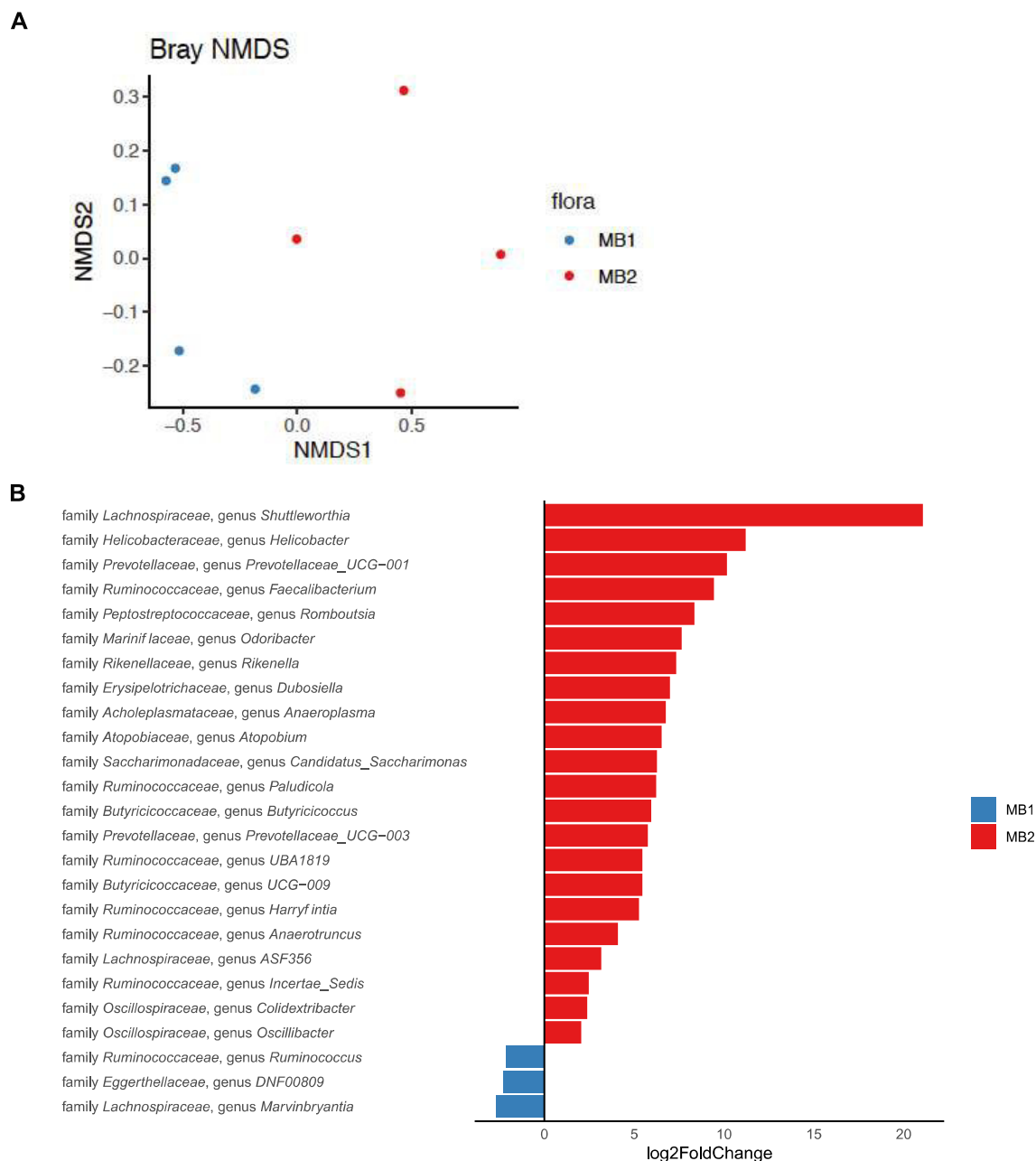


Figure S2: Microbiota profiling of MB1 and in colitogenic MB2. Wild-type mice bred under microbiota conditions 1 (MB1) and 2 (MB2) were sacrificed and stool samples from 4 mice were collected per group. Microbiota profiling was performed as described in the materials and methods. (A) PCoA of Bray-Curtis dissimilarities shows beta diversity across mice bred under MB1 and MB2 conditions. (B) Genera with significantly different abundance between groups.

Figure S2

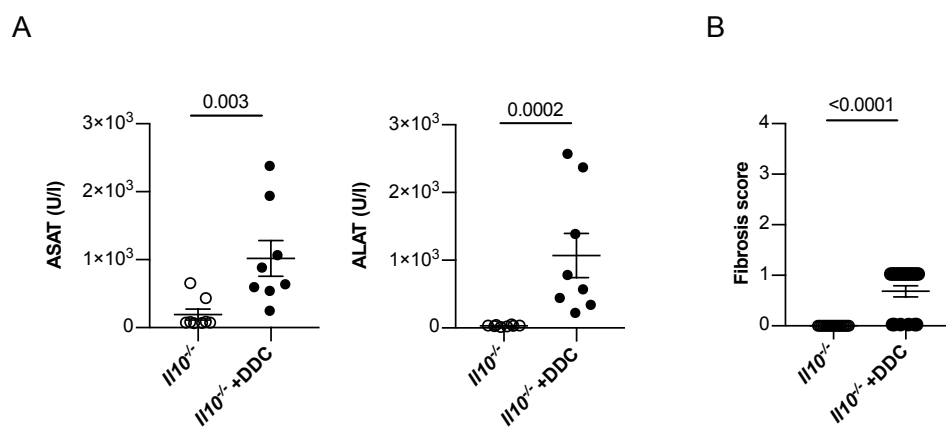


Figure S3: Liver inflammation in *Il10*^{-/-} mice after DDC-induced liver cholestasis. Liver cholestasis was induced by 2% DDC feeding in *Il10*^{-/-} mice gavaged with MB2, as described in Figure 2. After 9 days of feeding the mice with the DDC diet, mice were sacrificed and liver inflammation was analyzed by (A) serum Aspartate Aminotransferase (ASAT) and Alanine Aminotransferase (ALAT) (8= mice per group). (B) Fibrosis score was analyzed by Sirius Red staining. For statistical analysis, Mann-Whitney U test was performed.

Figure S3

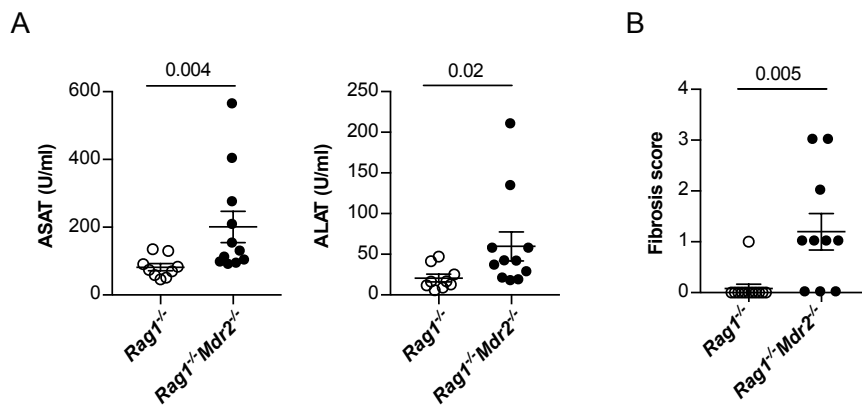


Figure S4: Liver inflammation in *Rag1*^{-/-}*Mdr2*^{-/-} mice after induction of Foxp3-CD45RB^{high} transfer colitis. Colitis was induced in *Rag1*^{-/-} and *Rag1*^{-/-}*Mdr2*^{-/-} mice upon transferring Foxp3-CD45RB^{high} cells, as described in Figure 3. On day 14, mice were sacrificed and liver inflammation was analyzed by (A) serum Aspartate Aminotransferase (ASAT) and Alanine Aminotransferase (ALAT) (n=9 *Rag1*^{-/-} n=11 *Rag1*^{-/-}*Mdr2*^{-/-}). (B) Fibrosis score was analyzed by Sirius Red staining. For statistical analysis, Mann-Whitney U test was performed.

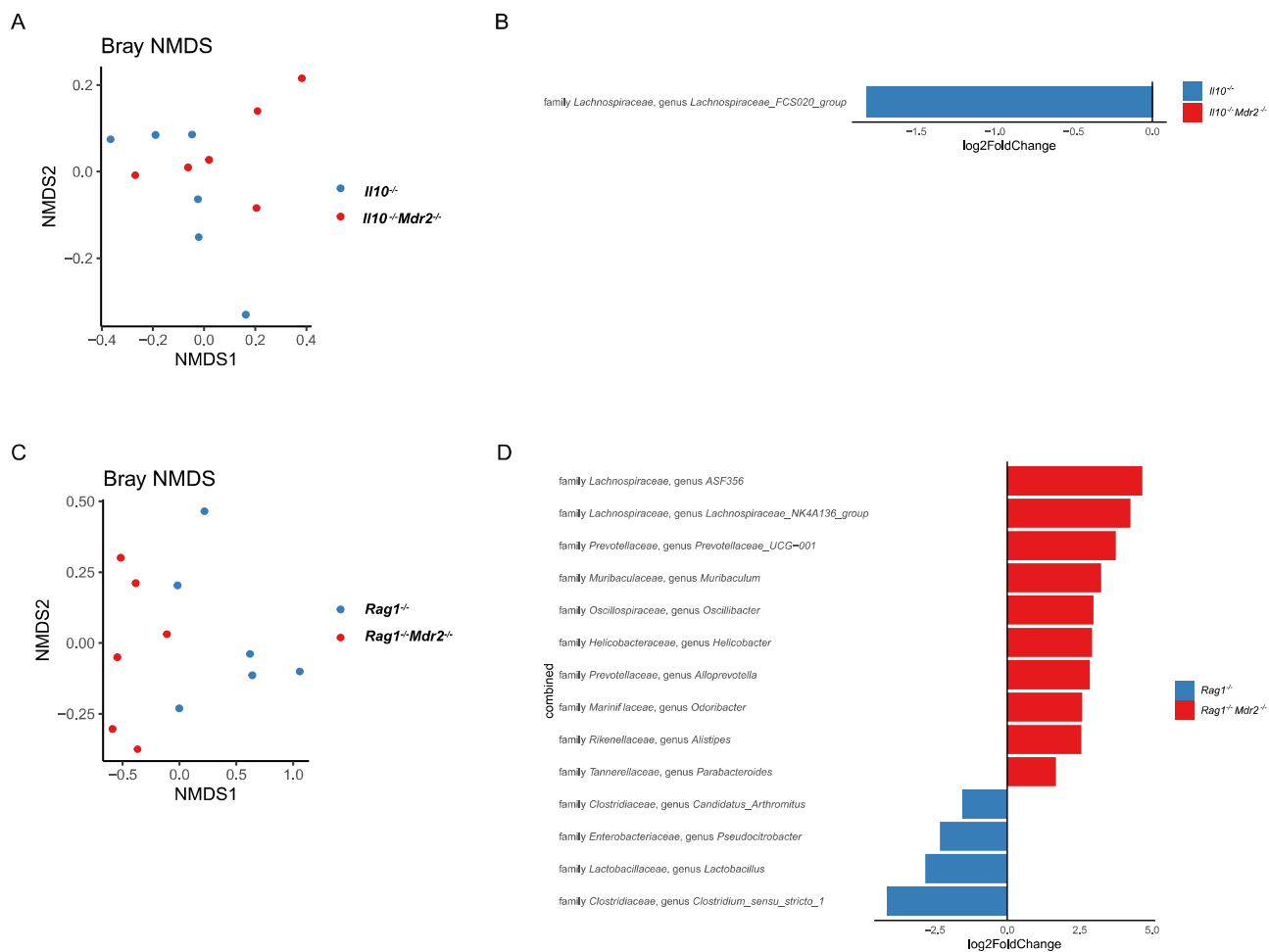


Figure S5: Concomitant liver inflammation alters the intestinal microbiota in *Il10*^{-/-} and *Rag1*^{-/-} mice suffering from colitis. *Il10*^{-/-}, *Il10*^{-/-}*Mdr2*^{-/-} mice (MB1) and *Rag1*^{-/-}, *Rag1*^{-/-}*Mdr2*^{-/-} mice (MB2) were sacrificed as described in Figures 1 and 3, respectively, and stool samples from 6 mice were collected per group. Microbiota profiling was performed as described in the materials and methods. (A) PCoA of Bray-Curtis dissimilarities shows beta diversity across *Il10*^{-/-} and *Il10*^{-/-}*Mdr2*^{-/-} mice. (B) Genera with significantly different abundances between groups. (C) PCoA of Bray-Curtis dissimilarities shows beta diversity across *Rag1*^{-/-} and *Rag1*^{-/-}*Mdr2*^{-/-} mice. (D) Genera with significantly different abundances between both groups.

Figure S5

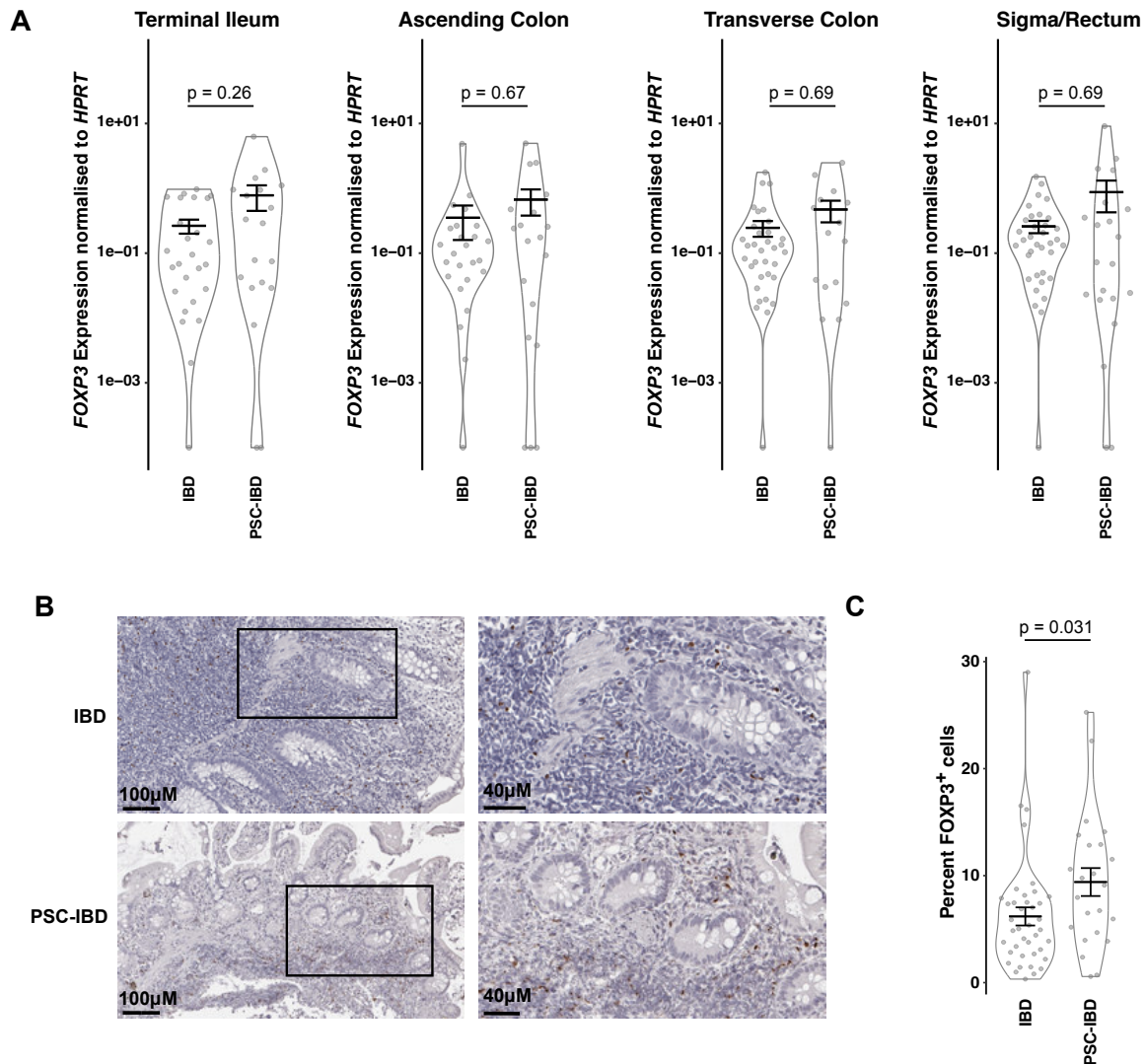


Figure S6: Increased FOXP3 protein expression in intestinal biopsies of people with PSC-IBD. (A) *FOXP3* mRNA expression levels were analyzed from intestinal biopsies taken from the terminal ileum, ascending colon, descending colon or sigma/rectum from every person with clinically active disease. (B) Representative images and (C) quantification of FOXP3⁺ cells in intestinal biopsies taken from the terminal ileum and sigma/rectum from every person with clinically active disease. To test for significance MLEM, post hoc Dunnett test was used.

Figure S6

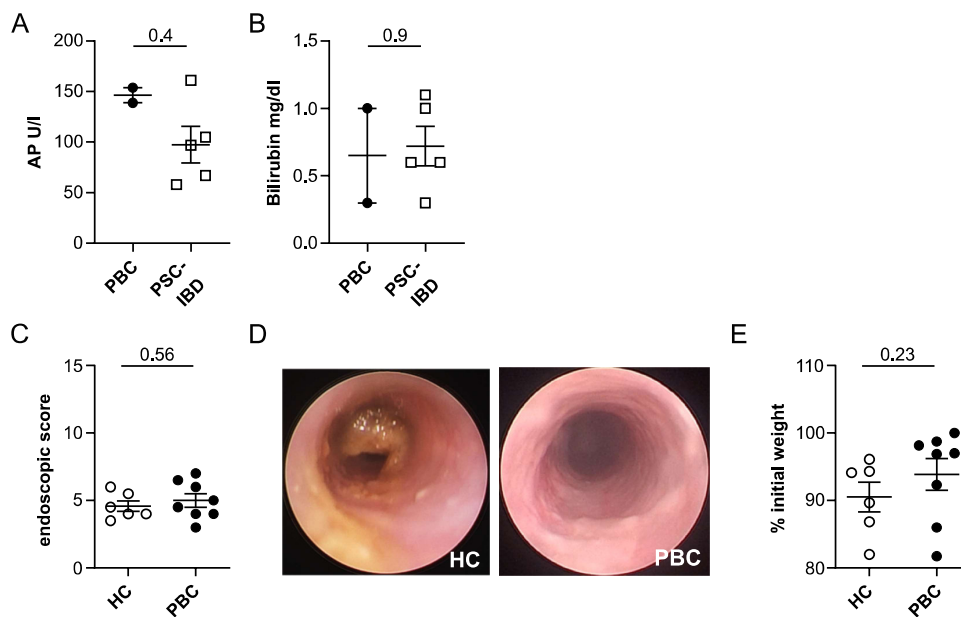


Figure S7: Colitis severity in germ-free mice is not affected by UDCA treatment of the stool donor. (A+B) People with PBC with comparable cholestasis to people with PSC-IBD were chosen. Stool transfer from healthy control (HC) and people with primary biliary cholangitis (PBC) that received UDCA treatment into germ-free mice before the chemical induction of colitis for 7 days. On day 9, colonic inflammation was analyzed by (C+D) colonoscopy as represented by endoscopic score and representative pictures and (E) weight loss. Each dot represents one mouse. For statistical analysis Mann-Whitney U test was performed.

Figure S7

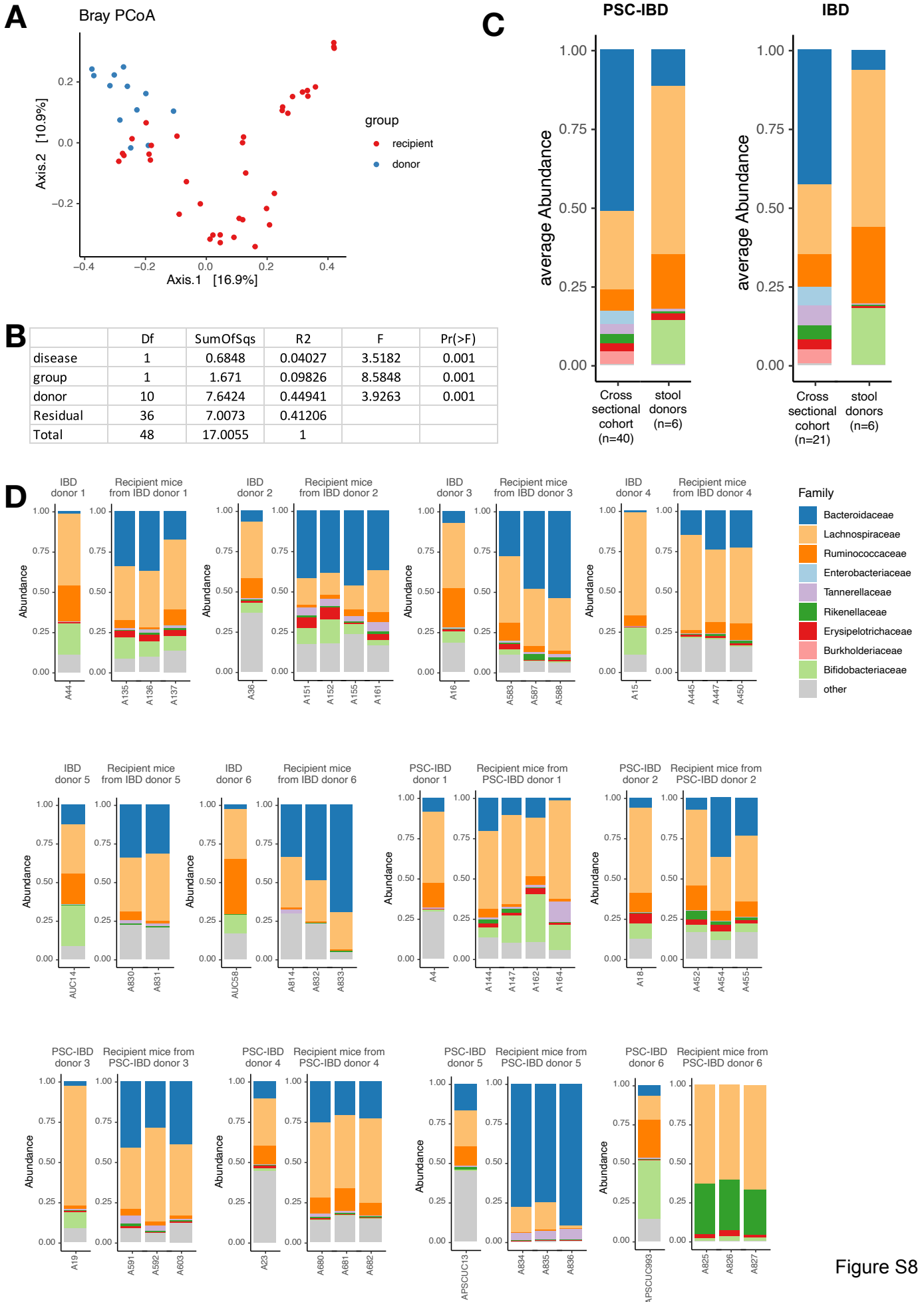


Figure S8

Figure S8: Microbiota profiling of stool from human donors and respective recipient mice. (A) PCoA of Bray-Curtis dissimilarities shows beta diversity across stool samples from human donors and recipient mice. (B) PERMANOVA analysis showing the contribution of disease, group (donor vs. recipient) and donor to the variation observed in the data shown in A. (C) A bar plot displaying the most abundant families, comparing a cross-section with the stool donors used in this study. (D) Abundance of the 10 highest abundant families across donor samples and their respective recipient mouse samples.

Table S1. Characteristics of microbiota donors.

	IBD	PSC-IBD	PBC
n-value	6	5	2
age in years	41±15.2	43±9.7	65±2.2
sex male (%)	4 (66%)	3 (60%)	2 (100%)
IBD disease activity, n (%)			
Remission	2 (33%)	3 (60%)	0 (0%)
Mild	2 (33%)	0 (0%)	0 (0%)
Moderate	1 (16%)	2 (40%)	0 (0%)
Severe	1 (16%)	0 (0%)	0 (0%)
Medications, n (%)			
5-ASA	4 (66%)	3 (60%)	0 (0%)
Thiopurines	2 (33%)	1 (20%)	0 (0%)
Anti-TNF	1 (16%)	2 (40%)	0 (0%)
Anti-IL12/23	1 (16%)	0 (0%)	0 (0%)
UDCA	0	5/5 (100%)	2/2 (100%)
Methotrexate	1 (16%)	0 (0%)	0 (0%)

*IBD disease activity was categorized based on Mayo score for UC (remission: 0-2, mild: 3-5, moderate: 6-10, severe 11-12 points).

Table S2. Characteristics of patients analyzed by immunohistochemistry

	IBD	PSC-IBD
n-value	30	19
age in years	42 ± 14.5	37 ± 14.5
sex male %	60%	84%
Disease activity, n (%)		
Remission	12 (40%)	9 (47%)
Mild	13 (43%)	7 (37%)
Moderate	3 (10%)	3 (16%)
Severe	2 (7%)	0
Medications, n (%)		
5-ASA	17 (57%)	6 (32%)
Thiopurines	2 (7%)	7 (37%)
Anti-TNF	14 (47%)	5 (26%)
Anti-IL12/23	1 (3%)	2 (11%)
UDCA	0	16 (84%)
Methotrexate	1 (3%)	0